https://doi.org/10.5194/bg-2021-23
Preprint. Discussion started: 12 May 2021

Biogeosciences Discussions

Labilization and diversification of pyrogenic dissolved organic matter by microbes

Aleksandar I. Goranov[1,*], Andrew S. Wozniak[2], Kyle W. Bostick[3,†], Andrew R. Zimmerman[3], Siddhartha Mitra[4], and Patrick G. Hatcher[1]

[1]Department of Chemistry and Biochemistry, Old Dominion University, Norfolk, VA, USA
[2]School of Marine Science and Policy, College of Earth, Ocean, and Environment, University of Delaware, ewes, DE, USA
[3]Department of Geological Sciences, University of Florida, Gainesville, FL, USA
[4]Department of Geological Sciences, East Carolina University, Greenville, NC, USA

Correspondence to: Patrick G. Hatcher (phatcher@odu.edu)

Abstract

With the increased occurrence of forest fires around the world, interest in the chemistry of pyrogenic organic matter (pyOM) and its fate in the environment has increased. Upon leaching from soils by rain events, significant amounts of dissolved pyOM (pyDOM) enter the aquatic environment and interact with microbial communities that are essential for cycling organic matter within the different biogeochemical cycles. To evaluate the bio-reactivity of pyDOM, aqueous extracts of laboratory-produced chars were incubated with soil microbes and the molecular changes to the composition of pyDOM were probed using ultrahigh resolution mass spectrometry (Fourier transform – ion cyclotron resonance – mass spectrometry). Given that photo-degradation also affects the composition and reactivity of pyDOM during terrigenous-to-marine export, the effects of photochemistry were also evaluated in the context of the bio-reactivity of pyDOM.

Ultrahigh resolution mass spectrometry revealed that, after incubation, many different (both aromatic and aliphatic) compounds were degraded, and new labile compounds, 22 – 40 % of which were peptide-like, were produced. This indicated that a portion of pyDOM has been labilized into microbial biomass during the incubations. Fluorescence excitation-emission matrix spectra revealed that some fraction of these new molecules is associated with fluorophores from proteinaceous and/or autochthonous/microbial biomass origin. Two-dimensional ^{1}H-^{1}H total correlation NMR spectroscopy identified a peptidoglycan-like backbone within the microbially produced compounds. These results are consistent with previous observations of nitrogen from peptidoglycans within the soil and ocean nitrogen cycles.

Interestingly, the exact nature of the bio-produced organic matter was found to vary drastically among samples indicating that the used microbial consortium may produce different exudates based on the composition of the initial pyDOM. Another potential explanation for the vast diversity of molecules is that microbes only consume low molecular weight compounds, but they also produce reactive oxygen species (ROS), which initiate oxidative and recombination reactions that produce new molecules. The observed microbially-mediated diversification of pyDOM suggests that pyDOM contributes to the observed large complexity of natural organic matter. More broadly, pyDOM can be substrate for microbial growth and be incorporated in environmental food webs.

1 Introduction

Pyrogenic organic matter (pyOM), the carbonaceous solid residue that is left after biomass burning (e.g., forest fires, biochar production), has been gaining attention in recent years as an important active component of

[*] Current Address: Department of Earth and Environmental Sciences, Rensselaer Polytechnic Institute, Troy, NY, USA
[†] Current Address: Fugro GeoServices, 6100 Hillcroft Avenue, Houston, TX, USA

https://doi.org/10.5194/bg-2021-23
Preprint. Discussion started: 12 May 2021

the global biogeochemical cycles. Compositionally, pyOM is mainly comprised of condensed aromatic compounds (ConAC) of various degrees of condensation and functionalization (Masiello, 2004; Schneider et al., 2010; Wagner et al., 2018). These molecules have been found in various environmental matrices such as soils and sediments (Schmidt and Noack, 2000; Skjemstad et al., 2002; Reisser et al., 2016) and atmospheric aerosols (Wozniak et al., 2008; Bao et al., 2017). In these environmental matrices, ConAC were originally thought to be exclusively stable ("recalcitrant") due to their highly condensed character (Goldberg, 1985; Masiello and Druffel, 1998). However, more and more studies report the presence of pyrogenic molecules in different aquatic environments (Hockaday et al., 2006; Dittmar and Paeng, 2009; Roebuck et al., 2017; Wagner et al., 2017; Li et al., 2019). These studies support the estimates that riverine systems annually export large amounts of pyrogenic dissolved organic matter (pyDOM) to the global ocean (Dittmar et al., 2012; Jaffé et al., 2013; Wang et al., 2016; Marques et al., 2017; Jones et al., 2020). During export, pyDOM is likely altered by various processes resulting in degradation and alteration of its physico-chemical characteristics (Masiello, 2004; Coppola et al., 2019; Wagner et al., 2019). Using laboratory-prepared chars and conservative assumptions, Bostick et al. (2018) approximated that 86% of the leached pyDOM is degradable (e.g., mineralizable to CO_2), which indicates that pyDOM is a very active component within the global carbon cycle, as previously suggested (Druffel, 2004; Lehmann, 2007; Riedel et al., 2016).

In sunlit aquatic environments, photo-degradation is the most significant sink for the ConAC fraction of pyDOM (Stubbins et al., 2012). The photochemistry of ConAC and pyDOM has been studied utilizing either laboratory-prepared pyDOM (Ward et al., 2014; Fu et al., 2016; Li et al., 2019; Bostick et al., 2020b; Goranov et al., 2020; Wang et al., 2020) or ConAC-rich natural organic matter (Stubbins et al., 2010, 2012; Wagner and Jaffé, 2015). These studies have reported that ConAC are exceptionally photo-labile and they degrade through a series of oxygenation, ring-opening, and decarboxylation reactions leading to a pool of smaller aliphatic by-products. Additionally, pyDOM photochemistry has been associated with the production of high fluxes of reactive oxygen species (ROS), important transients involved in the photo-degradation of pyDOM (Fu et al., 2016; Li et al., 2019; Goranov et al., 2020; Wang et al., 2020). These studies have contributed to a better understanding of the biogeochemical cycling of pyDOM in the presence of sunlight in the environment. Microbial (biotic) pathways are another degradative pathway with high potential for altering and/or mineralizing pyDOM, but they are far less understood.

Biotic reworking of organic molecules is a key mechanism for producing the diverse molecular composition of natural organic matter (Lechtenfeld et al., 2015; Hach et al., 2020). Due to the highly condensed character of pyOM, it is often regarded as bio-recalcitrant, though several studies have shown that a fraction (about 0.5 to 10 %) is indeed bio-degradable (Kuzyakov et al., 2009, 2014; Zimmerman, 2010; Zimmerman et al., 2011). PyOM is mainly comprised of ConAC (Bostick et al., 2018; Wozniak et al., 2020), which contributes to its low bio-degradability (Zimmerman, 2010). By contrast, pyDOM is highly heterogeneous (Wozniak et al., 2020), and in addition to ConAC, it contains numerous low molecular weight (LMW) species (e.g., acetate, methanol, formate; Bostick et al., 2018; Goranov et al., 2020) as well as various pyrogenic aliphatic compounds and inorganic nutrients (Hockaday et al., 2007; Mukherjee and Zimmerman, 2013; Goranov et al., 2020; Wozniak et al., 2020). The very solubility of pyDOM is imparted by the greater abundance of polar functional groups, which would also allow for greater microbial accessibility. To date, there is no study that evaluates the molecular-scale bio-degradability of pyDOM. It is unknown whether and how (e.g., mechanistic pathways, kinetic rates) these different compound groups are bio-degraded.

Additionally, there are concerns that leachates of fire-derived substances may be toxic due to the presence condensed and ligninaceous aromatics. It has been shown that cellulose- and pinewood-derived biochar water-extracts (pyDOM of laboratory-made charcoals) inhibit the growth of cyanobacteria while pyDOM of lignin-derived biochar has no inhibitory effects (Smith et al., 2016). The toxicity has been mainly attributed to polysubstituted phenols in the above-mentioned biochars. In natural systems, however, it is likely that other pyDOM components also play a role in controlling the bio-reactivity of pyDOM. An important very recent finding is that pyOM and pyDOM contain organochlorine compounds (both aliphatic and aromatic; Wozniak et al., 2020), which may enhance the toxicity of these pyrogenic substances. Thus, biotic incubations of pyDOM are needed to reveal if microbial growth can be sustained in a pyDOM/ConAC-rich environment.

https://doi.org/10.5194/bg-2021-23
Preprint. Discussion started: 12 May 2021


Biogeosciences Discussions

To explore these questions, we incubated aqueous biochar leachates with a soil-derived microbial consortium and evaluated the compositional changes to pyDOM using numerous analytical techniques. Laboratory-produced biochars can be considered model pyrogenic substances as they are similar to what is produced during forest fires in the environment (Santín et al., 2017) but have not experienced environmental aging which impacts their physico-chemical properties (Ascough et al., 2011). We have used oak wood because most of riverine dissolved organic matter (DOM) is exported from forested catchments (Hedges et al., 1997), and used two pyrolysis temperatures (400 and 650 ^{O}C) representative of forest fire temperatures (Santín et al., 2015, 2016). As photochemistry has been shown to increase the bio-lability of various types of DOM (Kieber et al., 1989; Lindell et al., 1995; Wetzel et al., 1995; Benner and Biddanda, 1998; Moran and Covert, 2003; Qualls and Richardson, 2003; Obernosterer and Benner, 2004; Abboudi et al., 2008; Chen and Jaffé, 2014; Antony et al., 2018), we also incubated pyDOM that had been photo-irradiated. Previous studies of these pyDOM samples showed significant compositional and structural changes after photo-irradiation, which certainly implies different bio-reactivity (Bostick et al., 2020b; Goranov et al., 2020).

In a parallel study of the same samples (Bostick et al., 2020a), we quantified the total organic carbon (TOC) loss, respired CO_2, as well as the changes to the bulk structural composition as determined by one-dimensional ^{1}H nuclear magnetic resonance (NMR) spectroscopy. Additionally, in that study, benzenepolycarboxylic acids (BPCA) molecular markers were used to quantify the changes specific to the condensed (ConAC) fraction of pyDOM. It was found that pyDOM leachates derived from biochars of higher pyrolysis temperature (650 ^{O}C) were less bio-degradable than those from lower temperature (400 ^{O}C) leachates, and photo-irradiation increased the bio-lability of pyDOM. Over the 96-day incubation, up to 48% of the carbon was respired to CO_2 following first-order kinetics, with LMW compounds (e.g., acetate, formate, methanol) being preferentially degraded. To elucidate the molecular-level changes taking place during the bio-incubation of pyDOM, and probe the various molecules that are being degraded or produced by soil biota, we examined these samples using ultrahigh resolution mass spectrometry (Fourier transform – ion cyclotron resonance – mass spectrometry, FT-ICR-MS), two-dimensional NMR, and fluorescence spectroscopy. The collective results from these two studies improve our understanding of the degradative pathways of pyDOM and ConAC in the environment and allow us to better interpret observations pertaining to terrigenous-to-marine transfers and global cycling of organic matter.

2 Materials and Methods

2.1 Preparation of pyDOM samples

Two biochars were prepared by heating laurel oak wood (*Quercus hemisphaerica*) under N_2 atmosphere at 400 and 650 ^{O}C for 3 hours. After grinding and sieving to particles of uniform size (0.25 - 2.00 mm), the chars were leached in 18.1 mΩ MilliQ laboratory-grade water (5 g in 500 mL) over 50 hours on a shaker table. The obtained pyDOM leachates, hereafter referred to as “Oak 400 Fresh” and “Oak 650 Fresh”, were filtered using 0.2 µm Millipore GSWP mixed cellulose ester filters. Physico-chemical characteristics of similarly-produced solid chars and their leachates were reported in several previous studies (Zimmerman, 2010; Mukherjee et al., 2011; Bostick et al., 2018; Wozniak et al., 2020). A fraction of each leachate was also subjected to photo-irradiation for 5 days in a custom-made solar simulator equipped with Q-Lab Corporation UV-A lamps (295 – 365 nm, λ_{MAX} = 340 nm, 40 watt) equivalent to natural photo-irradiation of 12 days. Photo-transformation rates, structural changes, photo-irradiation apparatus design, and other relevant information has been published previously (Bostick et al., 2020b; Goranov et al., 2020). Photo-irradiated pyDOM samples will be hereafter referred to as “Oak 400 Photo” and “Oak 650 Photo”. The four samples were diluted to a uniform TOC concentration of 4.7 mgC·L^{-1} prior to microbial incubation.

2.2 Incubation of pyDOM

https://doi.org/10.5194/bg-2021-23
Preprint. Discussion started: 12 May 2021

Microbial incubation was performed using a soil-derived microbial consortium as an inoculum. Soil from the Austin Cary Memorial Forest (Gainesville, FL) was chosen, because this area is frequently subjected to prescribed burns (Johns, 2016), and its soil microbes likely interact with pyOM and pyDOM on a regular basis. Taxonomic details of its soil microbial characteristics have been published previously (Khodadad et al., 2011). The collected soil was treated to remove roots and detritus, and its water-extract was centrifuged to obtain a pellet. The pellet was then dissolved in 10 mL MilliQ laboratory-grade water to obtain an inoculate, 100 □L of which was used to spike 50 mL of each pyDOM substrate. Additionally, microbial nutrients (KH_2PO_4 and $(NH_4)_2SO_4$) were provided following Zimmerman (2010) to support a healthy growth medium. Samples were incubated in gas-sealed amber vials on a shaker table at 28 ± 5 ^{O}C for 10 days in the dark. Using a double-needle assembly, CO_2-free air (Airgas, Zero) was flushed through the samples on days 0, 2, 5, and 10, which oxygenated the samples and removed dissolved inorganic carbon for its measurement, and is reported by Bostick et al. (2020a). A procedural blank and control samples were prepared in the exact same way but were poisoned with $HgCl_2$ immediately following the mixing of the different components (pyDOM, inoculate, nutrients). Additionally, a solution of sucrose (0.5 g $C_{12}H_{22}O_{11}$ in 40 mL MilliQ laboratory-grade water) was also incubated in the same manner. All incubated samples were poisoned with $HgCl_2$ to terminate microbial activity before shipment to Old Dominion University (Norfolk, VA) for spectroscopic and spectrometric analyses. Prior to spectroscopic analysis (see Sect. 2.3 below) or spectrometric analysis (see Sect. 2.4 below), samples were filtered using acid-washed 0.1 µm Teflon (PTFE) syringe filters. Further details about sample preparation can be found in the parallel study (Bostick et al., 2020a).

2.3 Analysis of chromophoric and fluorophoric dissolved organic matter

Chromophoric DOM (CDOM) measurements were performed on a Thermo Scientific Evolution 201 ultraviolet-visible (UV-VIS) spectrophotometer operated in a double-beam mode. A matched Starna quartz cuvette with MilliQ water was used as a reference during all spectral measurements. Spectra were recorded from 230 – 800 nm using a 1 nm step, 0.12 s integration time, and 500 nm/min scan speed. In addition to the double-beam referencing, the average noise in the 700-800 nm spectral region was subtracted from the spectra to correct for any instrument baseline drifts, temperature fluctuations, as well as scattering and refractive effects (Green and Blough, 1994; Helms et al., 2008). After consecutive procedural-blank corrections, the spectra (kept in decadic units) were normalized to the cuvette path length (1.0 cm) and the TOC content (in $mgC \cdot L^{-1}$) to convert them to specific absorbance ($L \cdot mgC^{-1} \cdot cm^{-1}$; Weishaar et al., 2003). CDOM was quantified by integrating the spectra from 250 – 450 nm (Helms et al., 2008) and is reported in $L \cdot mgC^{-1} \cdot cm^{-1} \cdot nm$ units.

Fluorophoric DOM (FDOM) measurements were performed on a Shimadzu RF-6000 spectrofluorometer operated in 3D acquisition mode. Samples were analyzed without dilution as no sample yielded absorbance at 230 nm above 0.07 (Miller et al., 2010). Samples were excited from 230 – 500 nm (5 nm step) and emission was recorded over 250 – 650 nm (5 nm step) to obtain excitation-emission matrices (EEMs). Additionally, five replicate water Raman scans were acquired on MilliQ water in 2D emission mode by exciting the sample at 350 nm and fluorescence intensity was monitored over 365 – 450 nm (0.5 nm steps). All measurements were done with 5 nm slit widths of the monochromators, 600 nm/min scan speed, and in high-sensitivity mode.

EEMs were processed in MATLAB using the drEEM toolbox (version 0.4.0.) using previously published routines (Murphy et al., 2010, 2013). Briefly, using the FDOMcorrrect.m function, the raw EEMs were adjusted for instrumental bias, blank-corrected using an EEM of the procedural blank, and scaled to adjust for any inner-filter effects using the raw UV-VIS spectra (Kothawala et al., 2013). This function also normalized the EEMs to Raman units (RU) after the area of the water Raman peak (peak maximum at 397 nm) had been determined by the ramanintegrationrange.m function (Murphy, 2011) on the averaged water Raman spectrum. The EEMs were then processed using the smootheem.m function to remove 1st and 2nd order Rayleigh signals and Raman scattering. EEMs are visualized and difference plots are generated using an in-house MATLAB script.

2.4 Fourier transform - ion cyclotron resonance - mass spectrometry (FT-ICR-MS)

https://doi.org/10.5194/bg-2021-23
Preprint. Discussion started: 12 May 2021

Procedural blank, control, and incubated samples were loaded onto solid-phase extraction cartridges (Agilent Technologies Bond Elut PPL, 100 mg styrene divinyl copolymer) as previously described (Dittmar et al., 2008). Cartridges were eluted with methanol (Fisher Scientific, Optima LC-MS grade) and infused into an Apollo II electrospray ionization (ESI) source interfaced with a Bruker Daltonics Apex Qe FT-ICR-MS operating at 10 T and housed in the College of Sciences Major Instrumentation Cluster (COSMIC) facility at Old Dominion University (Norfolk, VA). The instrument is externally calibrated daily with a polyethylene glycol standard, and a surrogate laboratory pyDOM standard was analyzed before and after pyDOM analyses to verify for the lack of instrumental drift. Additionally, an instrumental blank of methanol was analyzed between samples to verify for the absence of sample carryover. ESI spray voltages were optimized for each sample to assure for consistent spray currents among the samples. For each sample, 300 transients with a 4MWord time domain were collected, co-added, and the resultant free induction decay was zero-filled and sine-bell apodized. After fast Fourier transformation, internal calibration of the resultant mass spectra was performed using naturally abundant fatty acids, dicarboxylic acids, and compounds belonging to the CH_2-homologous series as previously described (Sleighter et al., 2008). Then, using an in-house MATLAB script, salt, blank, and isotopologue (^{13}C, ^{37}Cl) peaks were removed. Molecular formulas within ± 1 ppm error were assigned to FT-ICR-MS spectral peaks (S/N ≥ 3) using the Molecular Formula Calculator from the National High Magnetic Field Laboratory (Tallahassee, FL). Formula assignments were restricted to elemental composition of $^{12}C_{5\text{-}\infty}$, $^{1}H_{1\text{-}\infty}$, $^{14}N_{0\text{-}5}$,$^{16}O_{0\text{-}30}$, $^{32}S_{0\text{-}2}$, $^{31}P_{0\text{-}2}$, and $^{35}Cl_{0\text{-}4}$, and were refined using previously established rules (Stubbins et al., 2010). Any ambiguous peak assignments were refined by inclusion within homologous series (CH_2, H_2, COO, CH_2O, O_2, H_2O, NH_3, HCl) following Kujawinski and Behn (2006) and Koch et al. (2007). For all samples, at least 80% of the mass spectral peaks were assigned, and they accounted for at least 93% of the mass spectral magnitude.

Molecular composition was evaluated by plotting the molecular formulas on van Krevelen (vK) diagrams, scatterplots of the formulas' hydrogen to carbon (H/C) versus oxygen to carbon (O/C) ratios (Van Krevelen, 1950; Kim et al., 2003). Formulas were further categorized using the modified aromaticity index (AI_{MOD}), a proxy for the aromatic character of the associated molecule (Koch and Dittmar, 2006, 2016) and calculated as shown in Eq.1.

$$AI_{MOD} = \frac{1 + C - \frac{1}{2}O - S - \frac{1}{2}(N + P + H + Cl)}{C - \frac{1}{2}O - N - S - P} \quad \text{Eq. 1}$$

Formulas were classified as following: Condensed aromatic compounds (ConAC, $AI_{MOD} \geq 0.67$, number of C-atoms ≥ 15), aromatic ($0.67 < AI_{MOD} \leq 0.50$), olefinic/alicyclic ($0 < AI_{MOD} < 0.50$), and aliphatic ($AI_{MOD} = 0$). Additionally, N-containing formulas falling in the ranges of $1.5 \leq H/C \leq 2$ and $0.1 \leq O/C \leq 0.67$ were classified as peptide-like. Statistical evaluation of means was performed in MATLAB using the "anova1" function which performs one-way analysis of variance (ANOVA). Post-hoc Scheffé's assessments were performed using the "multcompare" function in the same software.

For the Kendrick Mass Defect (KMD) series analysis (described later in the manuscript), Kendrick Mass (KM) was first calculated using the molecular weight of each compound (i.e., calculated mass from its molecular formula) following Eq. 2. Then, the Kendrick Nominal Mass (KNM) was calculated as the rounded integer (no decimals) of the Kendrick Mass (KM) as shown in Eq. 3. The Kendrick Nominal Mass (KMD) is the difference between KM and KNM, i.e., the decimals (Eq. 4). This analysis was performed for oxygen (O), carbonyl (CO), and carboxyl (COO) series (S).

$$KM = \text{Molecular Weight} \times S \quad \text{Eq. 2}$$

$$\text{where } S = \frac{15.9949146}{16.0000000} \text{ for O series; } \frac{27.9949146}{28.0000000} \text{ for CO series; and } \frac{43.9898292}{44.0000000} \text{ for COO series}$$

https://doi.org/10.5194/bg-2021-23
Preprint. Discussion started: 12 May 2021

$$\mathrm{KNM} = \text{integer of } \mathrm{KM} \quad \text{Eq. 3}$$

$$\mathrm{KMD} = \mathrm{KM} - \mathrm{KNM} \quad \text{Eq. 4}$$

236
237 **2.5 Two-dimensional Nuclear Magnetic Resonance (NMR) spectroscopy**
238
239 One-dimensional ^{1}H NMR spectra of the samples of this project were published and evaluated in the
240 parallel study (Bostick et al., 2020a). For the study of this manuscript, a select sample was analyzed using two-
241 dimensional ^{1}H-^{1}H total correlation spectroscopy (TOCSY) to further evaluate several functional groups of
242 interest. Analyses were performed on a 400 MHz (9.4 Tesla) Bruker BioSpin AVANCE III spectrometer fitted
243 with a double-resonance broadband z-gradient inverse (BBI) probe in the COSMIC facility. Samples were
244 analyzed without pre-concentration and volumetrically diluted with deuterated water (D_2O, Acros Organics,
245 100% D) to obtain a 90:10 H_2O:D_2O solution. Further details of sample preparation and acquisition of 1D ^{1}H
246 spectra are published elsewhere (Bostick et al., 2020a). To obtain ultraclean NMR spectra, NMR tubes were
247 soaked with aqua regia, rinsed extensively with ultrapure water, and individually tested as blanks to verify that
248 no background peaks are present. While ^{1}H spectra were originally processed using an exponential multiplication
249 function (line broadening) of 5 Hz to obtain higher signal-to-noise for a more accurate and precise integration
250 (Bostick et al., 2020a), here they were re-processed using a multiplication function of 1.5 Hz to better observe the
251 splitting (multiplicity) patterns of the peaks of interest. TOCSY spectra were acquired using the phase-sensitive
252 gradient-enhanced mlevgpphw5 pulse program. It utilizes a 17-step Malcolm Levitt (MLEV-17) composite
253 scheme (Bax and Davis, 1985) for magnetization transfer between any coupled nuclear spins, and a W5-
254 WATERGATE element for water suppression (Liu et al., 1998). Both short-range and long-range spin-spin
255 couplings were observed using 30 ms and 100 ms mixing times, respectively. The data were then zero-filled to a
256 4096 x 1024 matrix and then fitted with a π/2-shifted (SSB = 2) sine-squared window function. Linear prediction
257 to 256 points was used in the F_1 dimension. All spectra were internally calibrated to the sharp distinguishable
258 methanol singlet at 3.34 ppm (Gottlieb et al., 1997), and then were phased and baseline-corrected. T_1-noise
259 removal was performed by calculating the positive projection of rows with no resonances and the summed
260 projections were subtracted from all rows in the spectrum (Klevit, 1985). The same procedure was performed for
261 all columns (F_2 dimension).
262
263 **3 Results**
264
265 **3.1 Molecular changes to pyDOM after microbial degradation**
266
267 Ultrahigh resolution mass spectrometric analysis of the bio-incubated and corresponding control pyDOM
268 leachates revealed significant changes in molecular composition after the 10-day incubation (Fig. 1). The
269 identified molecular formulas for these samples were classified into one of three groups using a presence-absence
270 approach (Stubbins et al., 2010; Sleighter et al., 2012). This approach identifies any common formulas among the
271 two samples being compared (control and bio-incubated), as well as any formulas that are unique to each sample.
272 It is important to note that the electrospray ionization (ESI) source is prone to biases, and the analytical window
273 of FT-ICR-MS depends most critically on it. Thus, it may not identify compounds that are present if they are not
274 ionizable (Stenson et al., 2002; Patriarca et al., 2020). Therefore, it is essential that observations by FT-ICR-MS
275 are always paired with supplementary quantitative techniques (optical analyses, NMR, etc.) in order to determine
276 if the identified trends are real or an artifact of ESI charge competition (D'Andrilli et al., 2020).
277
278
279

https://doi.org/10.5194/bg-2021-23
Preprint. Discussion started: 12 May 2021

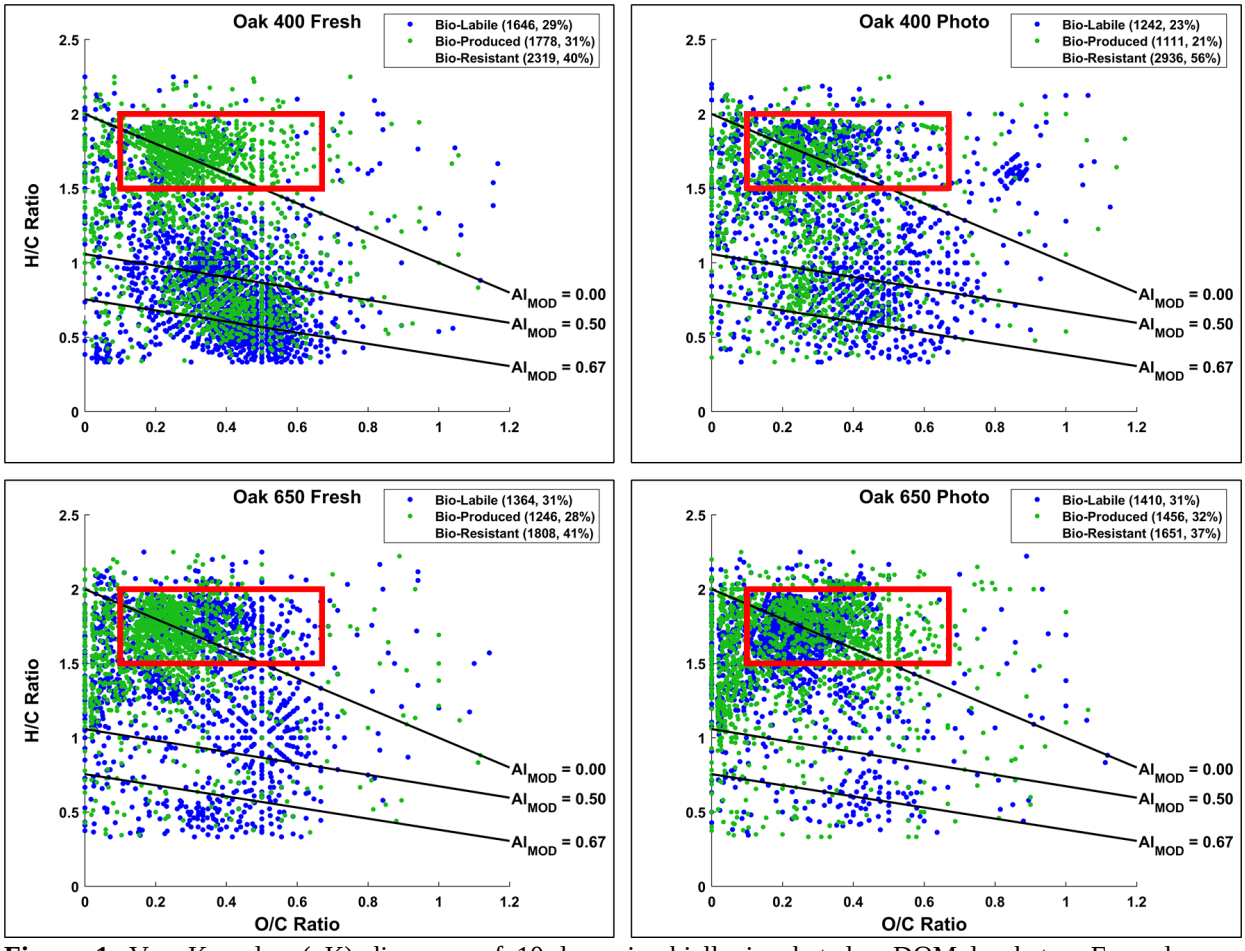

Figure 1. Van Krevelen (vK) diagrams of 10-day microbially incubated pyDOM leachates. Formulas are classified as **bio-labile** (molecular formulas only found in the "killed" control pyDOM leachates) and **bio-produced** (formulas that are only found in the bio-incubated samples). Formulas that are present in both the control and bio-incubated samples are operationally classified as bio-resistant and not shown for clarity. These three classes of molecules are separately plotted on vK diagrams and shown in Sect. 2 of the Supplement (Figs. S2-4). The number of formulas found in each of these pools is listed in the legends along with corresponding percentages (relative to total number of formulas in the two samples being compared). The black lines indicate modified aromaticity index cutoffs (AI_{MOD}; Koch and Dittmar, 2006, 2016), and the red box indicates the peptide region (valid only for N-containing formulas).

In all samples, nearly a third of the formulas (23 – 31%) present in the control samples were not observed after the biotic incubations, which is proportional to the organic carbon losses observed by Bostick et al. (2020a). Interestingly, for all leachates the degraded ("bio-labile") molecules were not from a specific area of the vK diagrams but rather represent a broad range of H/C and O/C ratios and compound types (see Fig. S2). This variety of compound characteristics among bio-labile molecules suggests that the degradation pathway may not be from microbial consumption alone. It would be unlikely for the soil microorganisms to utilize organic matter compounds as food indiscriminately. Most interestingly, it is evident that large numbers of aromatic ($AI_{MOD} \geq 0.50$) and some ConAC ($AI_{MOD} \geq 0.67$) formulas are lost, in agreement with observed losses in CDOM (Fig. S1 in the Supplement), as well as aryl functional groups (measured by ^{1}H NMR) and ConAC (measured by BPCA analysis) reported in the parallel study (Bostick et al., 2020a). Losses of specific compound classes, especially

https://doi.org/10.5194/bg-2021-23
Preprint. Discussion started: 12 May 2021

ConAC (due to their low ionizability) might be considered an artifact due to competition processes in the ESI source (Stenson et al., 2002; Patriarca et al., 2020. The agreement between FT-ICR-MS and other quantitative data (UV-VIS, NMR, TOC, BPCA) confirms the interpretation of degradation. Approximately half of the formulas (37 – 56%) in the original pyDOM leachates are classified, using the presence/absence approach, as bio-resistant (observed before and after biotic degradation). These formulas are located in all areas of the vK diagram (Fig. S3), showing variable oxygenation and aromaticity. Furthermore, the relative peak magnitudes of these formulas did not change significantly ($R^2 > 0.95$, Fig. S9; Sleighter et al., 2012), suggesting that a wide variety of pyDOM molecules appear to be recalcitrant to microbial degradation. Using the available molecular data, it is not possible to attribute the observed recalcitrance to any molecular property. Therefore, it is likely that some of these molecules are still bio-labile and would have degraded in due time if the incubations were sampled at later time points. Longer biotic incubations should be conducted in future studies to fully differentiate between labile and recalcitrant pyDOM molecules.

The use of hydrogen-to-carbon ratio (H/C) versus molecular weight (MW) plots has also been useful in interpreting ultrahigh resolution mass spectrometry data (e.g., Gonsior et al., 2018; Powers et al., 2019; Valle et al., 2020). Such graphs are presented using the presence-absence approach in Figs. S5-8 in Sect. 3 of the Supplement. These graphics help evaluate how different types of compounds (aliphatic vs aromatic) change relative to their MW. For both Oak 400 leachates, it is clear that large aromatic molecules (H/C < 1.5, MW > 550 Da) are removed during the biotic degradation, and smaller (300 < MW < 550) aromatic compounds are produced. These aromatic molecules that are being degraded into smaller ones are mainly ligninaceous and not ConAC, in agreement with the BPCA data published by Bostick et al. (2020a). With regards to the aliphatic molecules (H/C > 1.5), it is clear that molecules of a wide range of sizes are removed and created during the incubation suggesting that molecular weight is not a critical factor in their bio-lability. This is in apparent disagreement with the general knowledge that microbes preferentially consume low molecular weight substrates (e.g., Søndergaard and Middelboe, 1995), which was also concluded for these samples by Bostick et al. (2020a). The consumption of large molecules indicates that microbes utilize extracellular enzymes to degrade them into smaller substrates (Billen et al., 1990) or secondary degradative pathways are also at play.

3.2 Composition of bio-produced organic matter

The bio-produced organic compounds can be evaluated in various ways to examine the processes that may have occurred during the incubations. Using a presence/absence approach (Sleighter et al., 2012), the bio-produced formulas of each sample are compared with those of the other samples (Table 1). No significant overlap was found (2 – 320 formulas, 0 – 12%) among the molecules produced in the incubated pyDOM samples. Furthermore, no significant match was found between the bio-produced formulas of incubated pyDOM and those of the sucrose control sample (63 – 94 formulas, 3%, Table 1). These observations indicate that the products of the incubations were either vastly different for each sample and may depend on the starting substrate or were further altered post-exudation to result in their diversification.

Table 1. Overlap of bio-produced molecular formulas among samples. The number of formulas corresponds to the formulas in common between the two samples being compared, and the percentage is relative to the total number of formulas in the two formula sets.

Sample	Oak 400 Fresh	Oak 400 Photo	Oak 650 Fresh	Oak 650 Photo
Oak 400 Fresh	-	-	-	-
Oak 400 Photo	320 (12%)	-	-	-
Oak 650 Fresh	126 (4%)	104 (5%)	-	-
Oak 650 Photo	165 (5%)	81 (3%)	2 (0%)	-
Sucrose	94 (3%)	63 (3%)	68 (3%)	83 (3%)

https://doi.org/10.5194/bg-2021-23
Preprint. Discussion started: 12 May 2021

344 A significant fraction of the bio-produced organic matter was characterized as peptide-like (N-containing,
345 $1.5 \leq H/C \leq 2.0$, $0.1 \leq O/C \leq 0.67$). This indicates that microbes convert a part of pyDOM into labile DOM
346 (Moran et al., 2016; Vorobev et al., 2018), a process hereafter referred to as "microbial labilization". Given that
347 the pyDOM samples used in this study were poor in organic nitrogen, the microbes must have used the inorganic
348 nitrogen (NH_4^+) that was provided as a nutrient and converted some or all of it into microbial biomass. The
349 peptide-like microbially-produced formulas comprise 22 – 40 % of the bio-produced formulas (Table S2 in the
350 Supplement), and the results of the comparative analyses described above also imply that these proteinaceous
351 formulas are of highly variable composition. Their molecular diversity is additionally evaluated using one-way
352 analysis of variance (ANOVA) reported in Sect. 6 of the Supplement. This statistical tool indicated high molecular
353 variability supporting the findings by the presence/absence comparisons presented earlier (Table 1). The results
354 from these statistical assessments support the findings by the presence/absence comparisons and these findings
355 collectively conclude that the microbial incubations of pyDOM created pools of new, very diverse molecules, a
356 process hereafter referred to as "microbial diversification". As FT-ICR-MS was performed with soft electrospray
357 ionization with no fragmentation, the structure of the observed molecules is inferred from the elemental
358 composition of the assigned molecular formulas. Another possibility for these N-containing molecules is that they
359 were formed by radical processes that coupled pyDOM molecules with the NH_4^+ nutrient that was added to
360 support microbial growth. A preliminary experiment (data not shown) showed that mixing pyDOM with NH_4^+
361 did not result in abiotic formation of new molecules (for example via Michael addition; McKee et al., 2014), but
362 abiotic formation was not tested in the presence of radicals.
363 To confirm that these formulas were associated with proteinaceous structures and are not just N-containing
364 compounds that coincidentally plotted in the 'peptide region', spectrofluorometric analysis was performed to
365 obtain excitation-emission matrices (EEMs) of the pyDOM samples before and after bio-incubation (Fig. 2). The
366 data for Oak 650 Photo is not reported as the produced EEM spectra were of questionable quality, and as the
367 sample was in very limited amounts, analytical validation and quality assessment were not possible.
368

https://doi.org/10.5194/bg-2021-23
Preprint. Discussion started: 12 May 2021

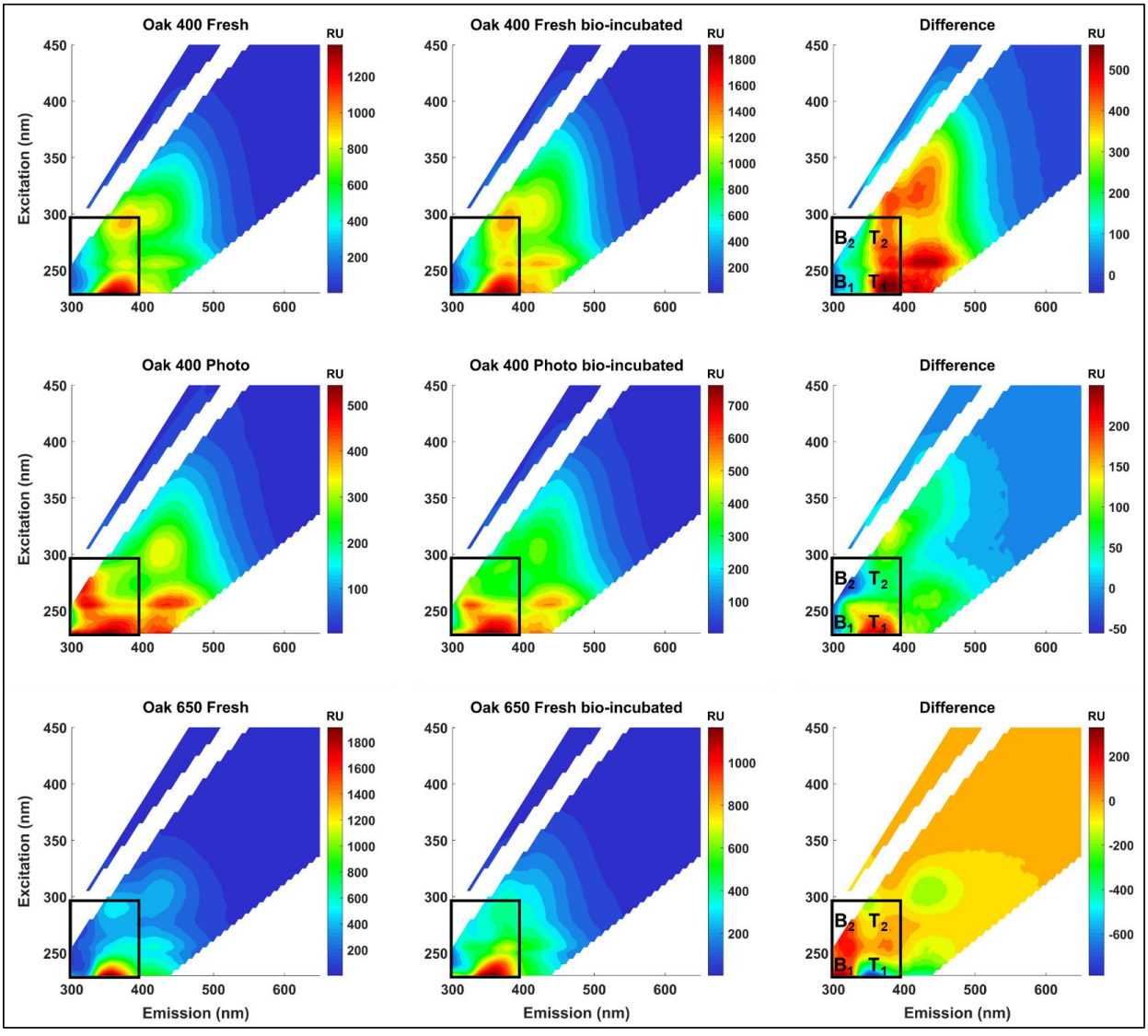

Figure 2. Fluorescence excitation-emission matrices (EEMs) of control (left panels) and bio-incubated (middle panels) pyDOM samples. Difference spectra are shown in the right panels. The black box indicates the region where compounds of proteinaceous and autochthonous/microbial origin fluoresce (Coble, 1996; Coble et al., 2014), with tyrosine-like (B_1 and B_2) and tryptophan-like (T_1 and T_2) peaks labeled on the difference plots (right panels).

Proteinaceous organic matter has a highly characteristic fluorophoric signature due to the distinguishable signals of the aromatic amino acids tyrosine and tryptophan. The short Stokes' shifts of these fluorophores allow them to spectroscopically separate on the EEM plot allowing for identification of related labile substances (Wünsch et al., 2019). Other amino acids, namely histidine and phenylalanine, are also fluorophoric, but are not easily identified in EEM data of complex matrices. A simplistic approach to evaluate the change after the bio-incubation is to use difference plots (e.g., Hemmler et al., 2019). For all samples, strong proteinaceous signals evolve after biotic incubations indicating that molecules of proteinaceous and autochthonous/microbial origin are produced (Coble, 1996; Coble et al., 2014). This indicated that peptide-like molecules observed using FT-ICR-

https://doi.org/10.5194/bg-2021-23
Preprint. Discussion started: 12 May 2021

MS are not an artifact due to charge competition in the source, but are truly bio-produced, validating the findings of the presence/absence analysis. There are subtle differences among the EEMs of all control and bio-incubated samples indicative of the high variability in fluorophoric content of these samples. This agrees with the observed variability in molecular composition described earlier. An interesting observation is that in the two Oak 400 pyDOM incubations, tyrosine-like fluorescence (peaks B_1 and B_2) decreases after biotic incubation while tryptophan fluorescence (peaks T_1 and T_2) increases. In contrast, the tryptophan-like fluorophores are degraded and tyrosine-like ones are produced after biotic incubation of Oak 650 Fresh pyDOM. It must be noted that there are proteinaceous fluorophores (and peptide-like formulas) in the control samples resulting from the addition of the microbial inoculate, but the associated fluorophores were present in low amounts. Thus, proteinaceous fluorescence signals in the control samples are not unexpected. However, a decrease in proteinaceous fluorophores is opposite of what is expected after significant microbial growth. Therefore, it is possibly due to fluorophoric compounds in this system being highly bio-labile and/or susceptible to oxidation by specific ROS, but the residual post-oxidation by-products would be still detectable by FT-ICR-MS and classified as peptide-like compounds. The loss of tyrosine-like fluorophores in the Oak 400 samples, and loss of tryptophan-like fluorophores in Oak 650 Fresh, are indicative of different microbial physiology and exudates in these incubations. The complexity of these EEM spectra and the compound-specific changes observed here indicate that proteomic and/or metabolomic analyses (e.g., Nalven et al., 2020) are necessary in future microbiological studies of pyDOM in order to fully understand the changes in molecular composition during such incubations.

To determine if the bio-produced formulas are from true proteins, or are compounds with residual proteinaceous fluorophores, the formulas were evaluated in the context of possible combinations of amino acids that would be singly charged. Given that microbes exude large proteins (molecular weight > 30 kDa) such as lignin peroxidases, manganese peroxidases, and laccases (Higuchi, 2004), the peptide-like formulas observed by FT-ICR-MS (analytical window of 200-1000 Da) may have resulted from hydrolysis of the above-mentioned enzymes (or other proteinaceous exudates). If that is the case, the hydrolysates would likely have had a simple oligomeric composition. To test this, the bio-produced peptide-like formulas in each sample were compared to a library of 888,009 possible combinations of 20 amino acids (oligomeric sequences of 2-7 residues). Only a small number of oligopeptides were identified (5 – 18 oligopeptides of 2 – 5 amino acids, Tables S2 and S3 in the Supplement) which is counter to the proposed idea that hydrolysis of microbial exudates produced these newly observed peptide-like formulas. The lack of identified oligopeptides also calls into question the idea that microbial processes were solely responsible for the high variability of the bio-produced organic matter observed after the microbial incubation of pyDOM.

In an attempt to further elucidate the composition of these bio-produced N-containing substances, we re-evaluated the previously published ^{1}H NMR data of these samples (Bostick et al., 2020a) in greater detail. Additionally, to further elucidate the connectivity between observed functional groups, two-dimensional ^{1}H-^{1}H total correlation NMR spectroscopy (TOCSY) was utilized on a select sample. Figure 3 shows the TOCSY spectra of the bio-incubated Oak 650 Fresh sample.

https://doi.org/10.5194/bg-2021-23
Preprint. Discussion started: 12 May 2021

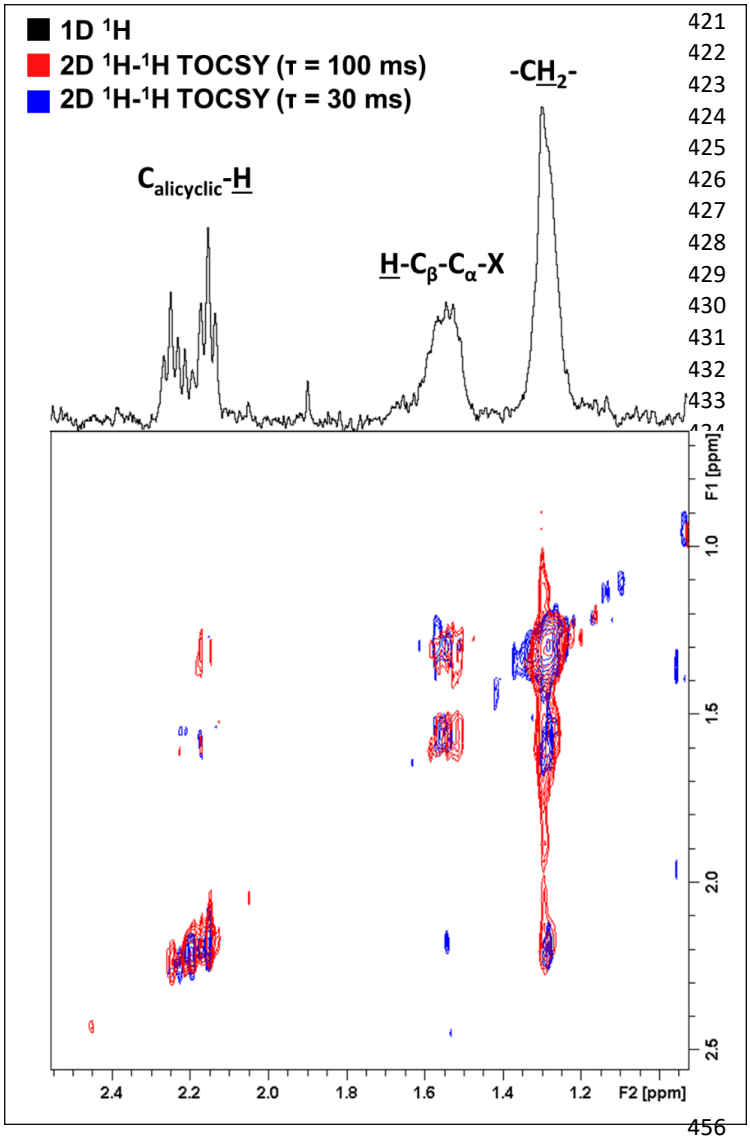

Figure 3. Two-dimensional ^{1}H-^{1}H total correlation spectroscopy (TOCSY) NMR spectra of the bio-incubated Oak 650 Fresh sample. Short- and long-range couplings were allowed to evolve during mixing times (τ) of 30 (**blue**) and 100 ms (**red**), respectively. The 1D ^{1}H spectrum is shown as a projection on top (**black**).

There are three groups of resonances that were found in all samples, even in the controls (although of small contributions relative to the total spectral signal). These resonances have not been previously observed in the ^{1}H NMR spectra of these pyDOM samples (Bostick et al., 2018; Goranov et al., 2020) indicating that they represent by-products of the microbial incubations, likely microbial biomass. In the control samples, the compounds associated with these resonances must be from the soil inoculant that was added. The three resonances are also observed to be in the same coupling network indicating that they are a part of the same or similar structures. Due to the very low concentration of these samples (3.5 – 4 mgC·L^{-1}), the NMR analysis did not allow for a high-resolution structural elucidation, but some distinct signatures were nonetheless observed. The deshielded aliphatic peaks at δ = 2.1 – 2.3 ppm have a complex multiplicity pattern, a characteristic feature of alicyclic structures. These are likely residual carbohydrate moieties which have lost most of their O-containing groups through various cleavage processes and their backbone $C_{alicyclic}$-**H** resonances have been shifted upfield. The peak at 1.55 ppm is from □-hydrogens to a heteroatom (**H**-C_{β}-C_{α}-X, where X = O, N, S), and these are known to be associated with peptidoglycans (Spence et al., 2011). The TOCSY analysis was performed with two different

https://doi.org/10.5194/bg-2021-23
Preprint. Discussion started: 12 May 2021

mixing times (τ = 30 and τ = 100 ms) in order to evaluate short-range (2 – 3 bond) and long-range (4 – 6 bond) connectivities. Based on the observed couplings the observed resonances are vicinal to each other (3 bonds away). This indicates that these functional groups are closely bound in the peptidoglycan substances they likely represent.

All of these analyses of the molecules observed after the biotic incubation of the four pyDOM samples conclude that the observed biochemical processes in these systems are complex and difficult to unambiguously interpret. Based on the findings above it is clear that these formulas can originate from three different sources:

1) exoenzymes, which microbes use to extracellularly degrade larger molecules into smaller ones (Hyde and Wood, 1997; Higuchi, 2004);
2) peptidoglycans, which likely leached into solution after bacterial death and cell lysis (Yavitt and Fahey, 1984); and
3) other metabolites and exudates involved in the physiology of the different microbes in the used consortium (e.g., signaling compounds).

The significant degradation of pyDOM and production of these biological compounds indicates that microbes successfully converted the presumably carbon-rich recalcitrant pyrogenic molecules into more labile substances, a process we hereafter refer to as "microbial labilization". However, the fact that the observed bio-produced labile molecules are not identifiable as simple oligopeptides, and are present in significantly different composition among the four samples, suggests that this molecular diversity may not be caused by predictable biotic reactions but by random radical-driven processes. Further evidence for the random radical-driven processes comes from the observed degradation of molecules across the whole vK space (Figs. 1 and S2), which is unusual because microbes generally preferentially consume smaller aliphatic species (Berggren et al., 2010a,b; Kirchman, 2018).

3.3 Radical oxygenation as a potential source of molecular diversity

Microbial physiology has been associated with the production of reactive oxygen species (ROS), which have been shown to be important in the degradation of various types of organic compounds (e.g., Scully et al., 2003; McNally et al., 2005; Porcal et al., 2013; Trusiak et al., 2018; Xiao et al., 2020). A recent study showed that radicals can degrade various types of ligninaceous molecules (Waggoner et al., 2017) suggesting that microbially induced radical reactions can target a variety of pyDOM molecules. While there were no ROS measurements made in this study, we have performed Kendrick Mass Defect (KMD) analysis of the FT-ICR-MS data (Kendrick, 1963; Hughey et al., 2001) to seek evidence for radical action. The KMD analysis identifies formulas that differ by any repeating structural moiety (e.g., -CH_2-). To identify potential products of radical attack, we have evaluated the FT-ICR-MS data in the context of oxygenation, i.e., searched the mass lists for formulas differing by one oxygen atom (addition of hydroxyl group), carbonyl group (addition of aldehydes or ketones), and carboxyl groups (Fig. 4).

https://doi.org/10.5194/bg-2021-23
Preprint. Discussion started: 12 May 2021

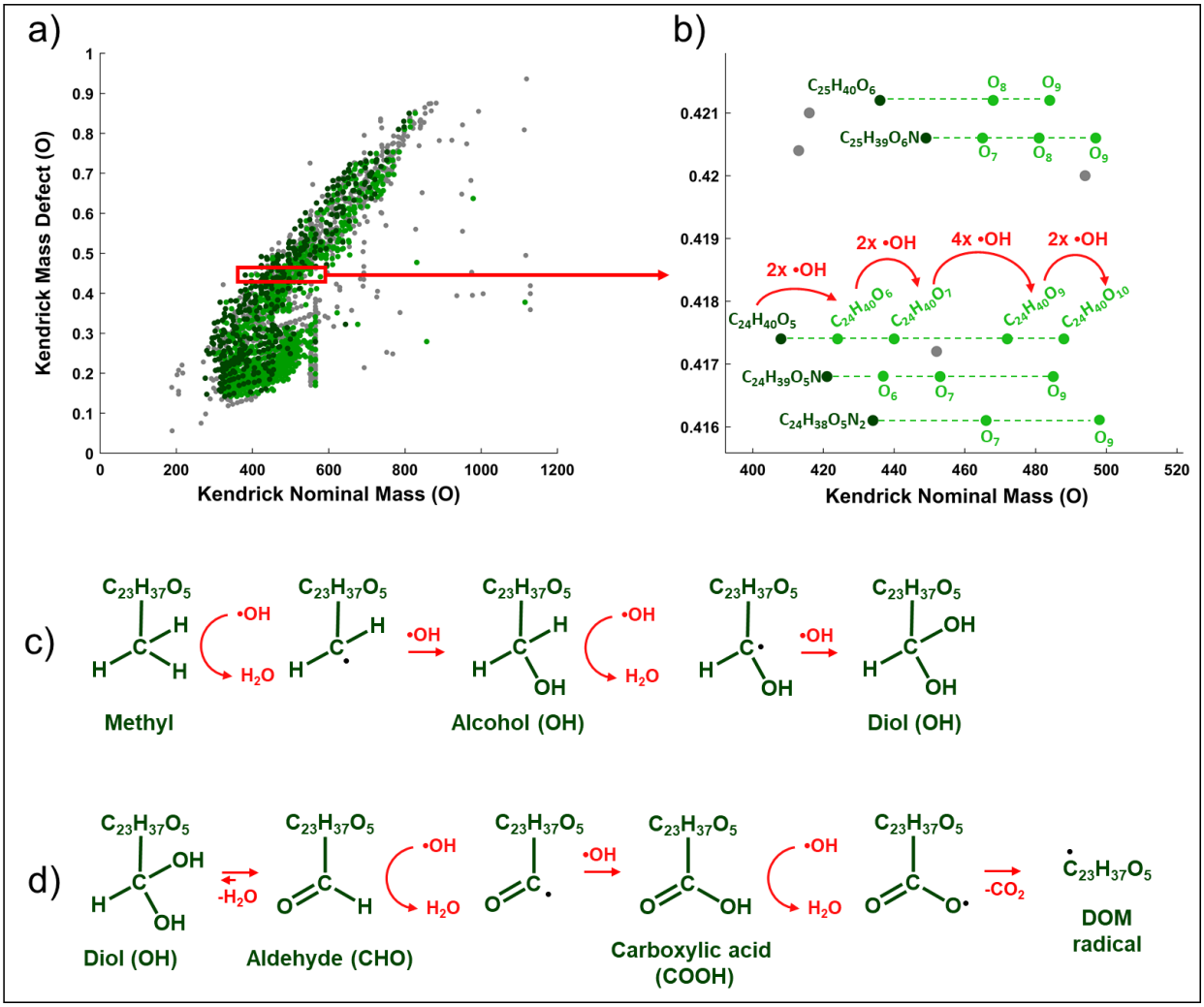

Figure 4. Kendrick Mass Defect (KMD) analysis using oxygen (O) series of the bio-produced formulas of Oak 400 Fresh pyDOM. Panel a) shows the whole KMD plot while panel b) shows an expanded region of it. Formulas not part of the O KMD series are colored in **gray**. Formulas in **dark green** are proposed substrates, and their oxygenation products are colored in **light green**. Only the molecular formulas for one of the series (KMD = 0.4174 Da) are labeled on panel b), while for the rest of the molecules, only the substrate formula and the number of oxygens in the oxygenation products are listed for clarity. The red arrows in panel b) show the formation of the four oxygenation products of the $C_{24}H_{40}O_5$ substrate after a sequential attack by hydroxyl radicals (•OH). Panel c) shows possible chemical reactions that can cause an increase of number of oxygens. Panel d) shows further oxidative processes involving the formation of keto and carboxyl groups which can contribute to the degradation of pyDOM, as well as to the formation of DOM. The KMD plots for all samples are shown on Figs. S10-12 in the Supplement.

The mathematics behind the KMD analysis (see Sect. 2.4) convert the mass of the molecular formula (also known as the IUPAC mass) to a "Kendrick" mass, whose mass is on a different scale which is specific for the selected structural moiety. On Fig. 4a, an example is shown with the KMD analysis for molecules differing by one oxygen (-O-). On the regular (IUPAC) mass scale, such formulas would differ by 15.994915 Da, but on the Kendrick "O" mass scale, they differ by 16 Da. The difference between the Kendrick Mass, KM (e.g., 408.2876

https://doi.org/10.5194/bg-2021-23
Preprint. Discussion started: 12 May 2021

Biogeosciences Discussions Open Access EGU

Da) and the Kendrick Nominal Mass, KNM (408 Da) is the Kendrick Mass Defect, KMD (i.e., 0.2876 Da), and formulas with the exact same KMD differ by one or more oxygens, and lie on a KMD series. Visually these formulas would plot on horizontal lines on the KMD plot as indicated by the dashed lines in Fig. 4b. Taking the series of KMD = 0.4174, this evaluation shows that there are five formulas in this particular KMD series that differ in number of oxygens ($C_{24}H_{40}O_{5\text{-}10}$). This implies that once $C_{25}H_{40}O_5$ is produced, it acts as a substrate and the other four formulas ($C_{24}H_{40}O_{6\text{-}10}$) are produced by oxygenation (likely in a sequential manner: $C_{24}H_{40}O_5 \rightarrow C_{24}H_{40}O_6 \rightarrow C_{24}H_{40}O_7 \rightarrow C_{24}H_{40}O_9 \rightarrow C_{24}H_{40}O_{10}$). This can happen via oxygenation by hydroxyl radical (•OH) attacks. This ROS can abstract a hydrogen from C-H bonds and the hydrogen is substituted with an OH-group, resulting in the formation of alcohols (C-OH) as shown in Fig. 4c. This is likely how the oxygenation products shown in Fig. 4a and 4b have formed. Evidence for such reactions will be found on the KMD plots as evolution of a new molecule within the same KMD series, but with a different number of oxygens. Further radical attack results in formation of polyols (Fig.4c). In the case of formation of geminal diols (two alcohol groups on the same carbon atom), they can rearrange to aldehydes or ketones via keto-enol tautomerism (Fig. 4d). Further radical attack would produce carboxyl groups, which can also be radically cleaved, and DOM radicals be formed. These radicals (as well as any other radical intermediate in this pathway) can be then further paired with hydrogen radicals (•H) from the solution, other •OH radicals, or other radicalized pyDOM or proteinaceous species.

Using KMD analysis, formulas produced by oxygenation were identified and plotted individually (Fig. 5). It is assumed that the smallest molecule in each series is the substrate and any molecules with more oxygens are oxygenation products.

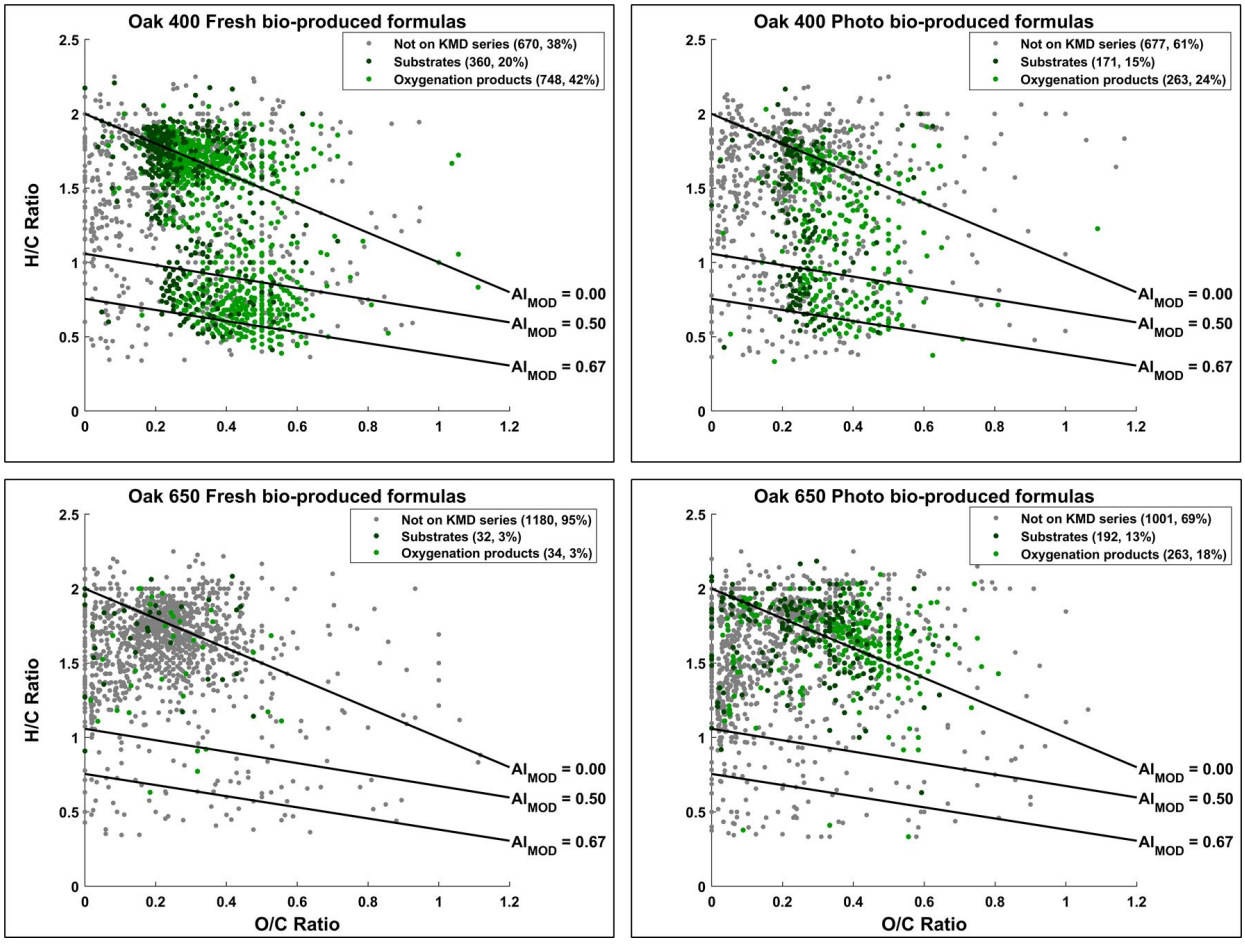

https://doi.org/10.5194/bg-2021-23
Preprint. Discussion started: 12 May 2021


Biogeosciences Discussions Open Access EGU

Figure 5. Van Krevelen diagrams evaluating oxygenation products among the bio-produced formulas of the four incubated pyDOM samples. Formulas not part of any of the oxygenation KMD series (O, CO, or COO) are colored in **gray**. Formulas in **dark green** are substrates with their oxygenation products colored in **light green**. The number of formulas in each of these pools are shown in the legends (along with corresponding percentages). The black lines indicate modified aromaticity index cutoffs (AI_{MOD}; Koch and Dittmar, 2006, 2016).

KMD analysis revealed that about a third (34 – 748, 3 – 42%) of the bio-produced formulas in these pyDOM samples could be classified as products of oxygenation reactions, likely driven by ROS species such as the hydroxyl radical (•OH). This is in agreement with previously observed cross-linking of microbial compounds through oxidative processes (Sun et al., 2017). The majority of the formulas, however, were not found to be products of oxidation as they did not lie on neither of the evaluated KMD series (O, CO, nor COO). Therefore, these compounds are likely formulas of exudates which were resistant to radical attacks or are formulas of compounds which have already been radically coupled with other compounds to result in unrecognizable molecules by the KMD analysis.

Additional evidence for intense radical processes in these systems is the evolution of bio-produced unsaturated aliphatic compounds ($1 < H/C < 2$, $O/C < 2$) on the vK diagrams (Figs. 1 and S4). ROS can attack aliphatic and aromatic compounds, open aromatic and alicyclic rings, cleave oxygen- or nitrogen-containing functionalities, and produce highly aliphatic molecules, as previously observed after photo-irradiation of pyDOM (Goranov et al., 2020), ConAC (Zeng et al., 2000a,b), and radical-based degradation studies of lignin (Waggoner et al., 2015, 2017; Waggoner and Hatcher, 2017; Khatami et al., 2019a, b). ROS can also attack any of the proteinaceous exudates and peptidoglycans cleaving them from many of their functional groups and converting them into the observed unsaturated aliphatic compounds. These produced aliphatic compounds could also contribute to the newly produced N-containing ("peptide-like") compounds observed by FT-ICR-MS if they are oxygenated by ROS post-formation. However, this seems unlikely as data from the supplementary fluorescence and NMR analyses support the formation of microbial biomass. These indirect observations of intense radical processes indicate that the microbial incubations of pyDOM are extremely complex systems, and future studies need to employ specialized more bio-analytical techniques to fully understand the processes occurring in them.

While FT-ICR-MS peak magnitudes are considered to be semi-quantitative, making it generally impossible to quantify the different bio-labile and bio-produced compounds, the ultrasensitivity of this technique ensures detection of all compounds that are within its analytical window. Here, the number of molecular formulas can be used as a quantitative measure for molecular diversity (e.g., Gurganus et al., 2015). Previously published liquid-state ^{1}H NMR data for the same samples (Bostick et al., 2020a) provide a quantitative measure of functional group content. Strong positive and negative correlations were observed between the numbers of bio-labile and bio-produced formulas and the percent NMR spectral signal accounted for by olefinic functionalities and methanol, respectively (Fig. 6 and Table S4). These correlations suggest that the diversity of bio-degraded (bio-labile) and bio-produce molecules was related in some way with a process related to the availability of methanol (CH_3OH) and olefinic functionalities (C=C) in pyDOM.

https://doi.org/10.5194/bg-2021-23
Preprint. Discussion started: 12 May 2021

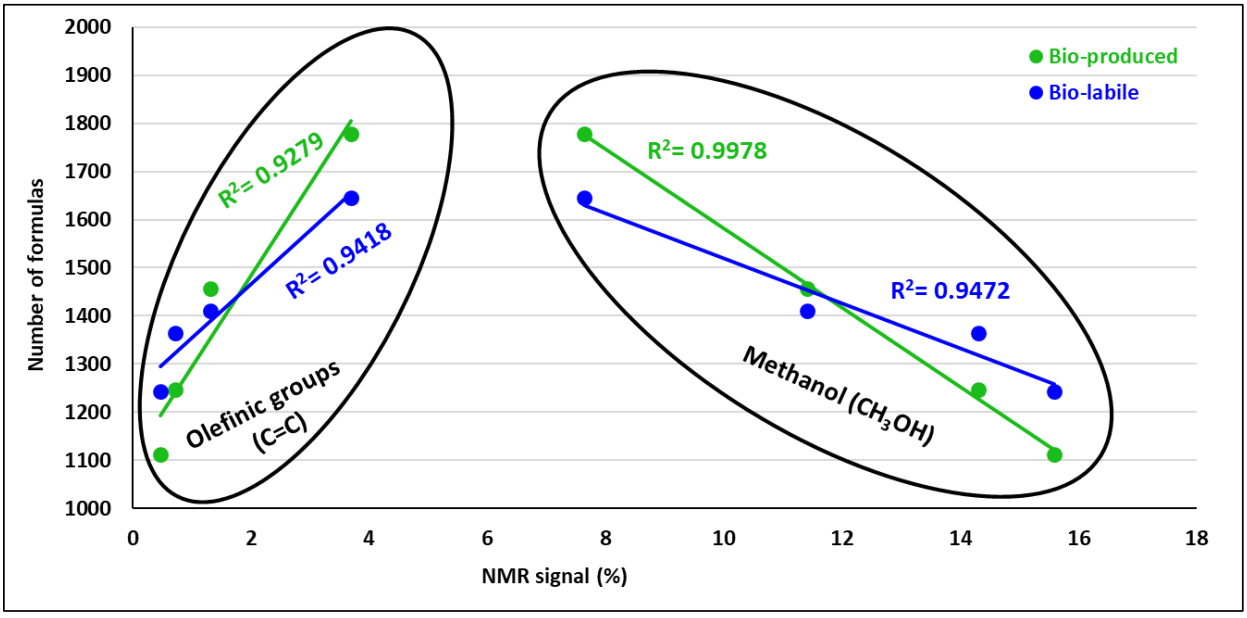

Figure 6. Correlation analysis between the number of **bio-labile** and **bio-produced** formulas detected by FT-ICR-MS and relative intensity (in %) of olefinic functionalities (C=C) and methanol (CH_3OH) as measured by liquid-state ^1H NMR and reported by Bostick et al. (2020a). No significant correlations were found between other functional groups and the number of bio-produced or bio-labile formulas (data shown in Table S4 of the Supplement).

Olefinic functionalities have been recently identified as important structural motifs in the composition of pyDOM and were observed to degrade in photochemical experiments due to their high reactivity with ROS species (Goranov et al., 2020). Although they are in low abundance in pyDOM (< 10%), it is likely they act as important intermediates in the degradative pathways of pyDOM. The olefinic bonds can be homolytically cleaved when attacked by radicals and effectively act as radical-accelerators that further propagate radical-mediated organic matter transformations. Thus, the abundance of olefins can further increase the abundance of radicals and contribute to the elevated molecular diversity resulting in the linear relationship shown in Fig. 6.

The other correlation between molecular diversity and NMR data is observed to be with methanol (CH_3OH), a very sharp highly distinguishable singlet at $\delta = 3.34$ ppm in ^1H NMR spectra (Gottlieb et al., 1997). As it is a common contaminant in NMR analysis, special precautions were taken to obtain ultraclean spectra (see Sect. 2.5). Methanol is a species that is naturally present in pyDOM (Bostick et al., 2018), and while it is generally considered to be toxic to microbes (Dyrda et al., 2019), there are methylotrophic bacteria and fungi (microbes of the families *methylococcaceae* and *methylobacteriaceae*) that can utilize it as a substrate (Chistoserdova et al., 2003; Kolb and Stacheter, 2013; Chistoserdova and Kalyuzhnaya, 2018). These species have been previously observed in the soil from the area where the microbial inoculum was extracted from (Khodadad et al., 2011), suggesting that the degradation of methanol may be biotic. In fact, in these samples, methanol, along with the other two measured low molecular weight substances, acetate and formate, was nearly completely degraded over the 10-day incubation (Bostick et al., 2020a).

The inverse relationship between the content of methanol and molecular diversity (Fig. 6) can be interpreted in several ways. Firstly, methanol could be exhibiting toxicity to the microbes that assimilate pyDOM, as has been observed previously (Dyrda et al., 2019). This, however, is unlikely for the pyDOM systems studied here because the sample with the highest amount of methanol (Oak 400 Photo, ~3.7% CH_3OH) was the second most bio-reactive (Bostick et al., 2020a). Instead, the observed strong negative correlation may be explained by the fact that methanol is a known radical-scavenger (Múčka et al., 2013). If, as we propose, the molecular diversity

https://doi.org/10.5194/bg-2021-23
Preprint. Discussion started: 12 May 2021

results from the activity of radical processes, an increasing concentration of methanol would quench these radicals thereby decreasing their activity and limiting the molecular diversity. This would explain the negative relationship depicted by the correlation shown in Fig. 6.

4 Discussion

4.1 Multiple pathways for the alteration of pyDOM by microbes

Using a variety of analytical platforms in this and the parallel study (Bostick et al., 2020a), significant quantitative and qualitative losses were observed when pyDOM was subjected to incubation with a microbial consortium collected from a site impacted by forest fires. Additionally, labile and diverse compounds were produced during these incubations. Due to the high complexity of pyDOM, the changes are not straightforward, and there are at least two important pathways at play, 1) degradation through microbial assimilation (consumption of pyDOM), and 2) degradation/transformation via radical-mediated reactions (e.g., oxygenation) by ROS produced from microbial exoenzymes. These two pathways are discussed in the context of degradation of pyDOM and formation of new labile and diverse molecules.

4.1.1 Molecular degradation of pyDOM

A surprising observation in this study is that there was a uniform loss of pyDOM molecules from all regions of the vK diagrams. Microbes, it is generally presumed, preferentially assimilate small non-aromatic substances such as carbohydrates, proteins, low molecular weight acids (Berggren et al., 2010a,b; Kirchman, 2018). Thus, the aromatic fraction of pyDOM, mainly the ConAC, are generally considered to be bio-recalcitrant (Goldberg, 1985; Masiello, 2004). In addition to the condensed character of many of the molecules, there are significant numbers of potentially toxic organochlorine compounds, of both aliphatic and aromatic character, in pyDOM (Wozniak et al., 2020). Thus, the finding of the major biological activity in these samples and the significant amount of carbon, including aromatic carbon, that was mineralized, is a very significant finding for the wildfire biogeochemistry community (Bostick et al., 2020a).

Although pyDOM is highly heterogeneous (Wozniak et al., 2020), the observation of diverse molecular consumption is not unique to it. In a recent microbial degradation study of snow DOM, Antony et al. (2017) observed that both aromatic (including ConAC, lignin, and tannins) and aliphatic formulas were bio-degraded. This is likely due to microbes evolving chemical mechanisms to thrive in the extreme conditions of glaciers (Antony et al., 2016). Analogously, as there have been previous prescribed fires in the area from which the microbes for this study were extracted (Johns, 2016), it is also possible that our organisms have adapted to the presence of ConAC and other pyrogenic substances, developing mechanisms for their assimilation (Judd et al., 2007).

While microbial assimilation of pyDOM compounds certainly occurred, our molecular data show that there was a second degradative pathway which likely contributed to the extensive molecular alteration, and to the significant loss of carbon that was quantified in the parallel study (Bostick et al., 2020a). While some microbial exoenzymes operate via hydrolytic pathways (amylases, lipases, proteases, cellulases, β-galactosidases, etc.), many other enzymes operate through oxidative (electron-withdrawing) pathways. Examples of such enzymes are the various lignin-modifying enzymes in the peroxidase (lignin peroxidases, manganese peroxidases, etc.) and phenoloxidase (e.g., laccases) families (Higuchi, 2004). Thus, reactive oxygen species are usually produced and involved in the microbial degradation of organic matter in the environment.

The bio-labile molecules in the studied pyDOM samples are of highly variable degree of oxygenation, aromaticity, and size (some MW > 550 Da). Thus, microbial exoenzymes would have been needed to reduce the size of substrates into smaller units that could pass through microbial cell membranes (Sinsabaugh et al., 1997; Fuchs et al., 2011; Burns et al., 2013) and be consumed by the biota. The presence of enzymatic compounds is confirmed by observation of peptide-like compounds (FT-ICR-MS analysis) and proteinaceous fluorophores (spectrofluorometric analysis). An important finding is that a preferential degradation of ConAC of smaller

https://doi.org/10.5194/bg-2021-23
Preprint. Discussion started: 12 May 2021

molecular weights was observed (Bostick et al., 2020a). As small ConAC (i.e., oxygenated PAHs) are known to be toxic (e.g., Idowu et al., 2019), it is unlikely that they were directly consumed by the microbes. These substances are highly susceptible to attacks by ROS, which is likely how they were degraded in these samples. Thus, we speculate that microbes are most likely not directly consuming ConAC, but rather, are degrading them indirectly using ROS. These radicals can oxygenate pyDOM with various functional groups (e.g., hydroxy, aldehyde/keto, carboxyl), and can also cleave functional groups (e.g., methoxy functionalities), open aromatic rings, and completely mineralize compounds to inorganic carbon (CO, CO_2, HCO_3^- and CO_3^{2-}) as shown on Fig. 4. ROS have been previously shown to be very important in pyDOM photochemistry (Ward et al., 2014; Fu et al., 2016; Goranov et al., 2020; Wang et al., 2020), and it is likely that they play an important role in the microbial degradation of pyDOM as well.

More evidence for radical species involvement is provided by the peptidoglycan molecules produced during pyDOM incubation. While these molecules are generally large (Vollmer et al., 2008) and would not be detected as singly-charged molecules using FT-ICR-MS (analytical window covering m/z 200-1000), their hydrolytic products (small oligopeptides) would be observed. Very few peptide sequences (5 – 18 oligopeptides of 2 – 5 residues) were identified among the bio-produced formulas indicating that such hydrolysates did not exist in the samples at the time of measurement. However, if there were abundant radical reactions occurring in the system, as we suggest, it is very possible that these hydrolysates were altered into unrecognizable organic structures that would still be classified as "peptide-like" but would have different molecular composition than the predicted linear peptide sequences. It is also possible that instead of peptidoglycan hydrolysis followed by consecutive oxygenation, ROS directly cleaved the peptidoglycans into smaller substances of peptide-like molecular composition.

4.1.2 Labilization and Diversification of pyDOM

The production of labile unrecognizable biological substances during these incubations correlates well with previous findings showing the formation of thousands of new biological compounds during biotic incubations unrelated to microbial metabolic pathways (Lechtenfeld et al., 2015; Wienhausen et al., 2017). However, in difference with previous studies, an insignificant overlap of bio-produced formulas was observed among the four pyDOM samples after the incubations (2 – 320 formulas, 0 – 12%). Insignificant numbers of matching formulas from pyDOM were also found in the bio-produced formulas of an incubation of sucrose with the same soil microbes (63 – 94 formulas, 3%). This indicates that microbes diversified the composition of these pyDOM samples.

The observed diversity can be explained by a scenario wherein the microbes secreted labile molecules whose identities differed depending on the growth medium and/or food source, yielding high variability among bio-produced formulas after the incubation of pyDOM. Additionally, it is possible that different microbial species (different bacteria, fungi, archaea, etc.) have proliferated in response to the sample-specific pyDOM composition, yielding different microbial populations growing during each different incubation, sequentially producing different bio-produced compounds (Fitch et al., 2018).

The finding of extreme molecular diversity contrasts with previous observations made by Lechtenfeld et al. (2015) in a study evaluating the molecular composition of microbially produced DOM. In their study, marine microbes were supplied with two different substrates (glucose and glutamic acid; and a mixture of oligosaccharides and oligopeptides), and a significant overlap (67 – 69 %) in the bio-produced organic matter was observed. The difference in observations between the work presented in this manuscript and by Lechtenfeld et al. (2015) is likely caused by a large difference in the composition of the pyDOM substrates relative to those in the Lechtenfeld et al. (2015) study. While the four pyDOM samples used here are highly heterogeneous to one another (Goranov et al., 2020; Wozniak et al., 2020), the substrates by Lechtenfeld et al. (2015) were of much higher similarity. Another possible reason is that the physiology of the soil microbes used here may be producing more diverse molecules than the marine microbes used by Lechtenfeld et al. (2015). It is likely that that aquatic microbes have a much different degradation strategy. As soils are far less rich in labile molecules, it is possible that soil microbes have adapted to produce much higher fluxes of ROS to degrade the more recalcitrant soil

https://doi.org/10.5194/bg-2021-23
Preprint. Discussion started: 12 May 2021

organic matter, which can also explain the larger dissimilarity in bio-produced organic molecules after the incubations of pyDOM.

An important observation using the H/C vs molecular weight plots (Fig. S5) was that the bio-produced compounds after incubation of pyDOM were of various molecular weights. Thus, it is likely that that the microbial biomass produced during the incubation is radically coupled with pyDOM molecules. This has been recently proposed as an important process in marine DOM cycling (Hach et al., 2020). In that study, when isotopically ^{13}C-labeled organisms were incubated with oceanic surface waters, microbially produced compounds were quickly coupled to the ambient marine DOM molecules. This "recombination" process occurred within hours of the production of microbial exudates, followed by the observation of a highly diversified DOM pool. This process is likely driven by radical coupling reactions, and such pathways have also been observed in incubations in the presence of sunlight (Sun et al., 2017). Another possible explanation is that chemically reactive species, such as quinones, reacted with microbially produced compounds via nucleophile-driven reactions (such as the Michael addition; McKee et al., 2014) to produce highly diverse pools of molecules after each incubation.

The observations from this study are compared to previous work by Waggoner et al. (2017) where a ligninaceous sample was treated with three different ROS: hydroxyl radical (•OH), singlet oxygen ($^1O_2$), and superoxide ($O_2^{\bullet-}$). Each different radical degraded a specific pool of ligninaceous compounds, which showed that different ROS can degrade a variety of types of organic matter. However, there was a significant overlap observed between the three pools of molecules that were degraded indicating that degradation pathways solely based on ROS attacks are still ordered. Thus, because ROS on their own do not produce completely diversified molecular pools, the combination of the two pathways we describe here must have occurred to produce the great variability in the bio-produced microbial biomass observed in our study.

Clearly, the chemistry behind these microbially induced compositional changes of pyDOM is highly complex, and the observed molecular diversity after these biotic incubations contrasts with previous studies. These discrepancies cannot be interpreted unambiguously using the employed analytical approaches, and future studies need to involve measurements of radicals and their effects, as well as various DNA sequencing and "omics" approaches.

4.2 Implications for the cycling of pyDOM in the environment

The present study provides a detailed evaluation of the compounds that microbes degrade and produce in samples mimicking pyDOM in hydrologically dynamic environmental systems such as riverine and groundwater systems. It brings new knowledge about the properties and reactivity of pyDOM and challenges the conventional idea that pyDOM is stable towards biotic degradation. Several studies have already shown that pyrogenic substances have soluble DOM components (Hockaday et al., 2007; Mukherjee and Zimmerman, 2013; Wagner et al., 2017; Bostick et al., 2018) and that more soluble components are produced with environmental aging (Abiven et al., 2011; Ascough et al., 2011; Roebuck et al., 2017; Quan et al., 2020). A recent study incubated pyDOM using riverine microbes and observed a significant degree of degradation as well (Qi et al., 2020). However, rather than using an extracted inoculate, in that work, the authors directly incubated pyOM in riverine water. Therefore, these incubations can be considered primed by the more labile riverine molecules (Guenet et al., 2010; Bianchi, 2011). The experiments presented in our study, in parallel with Bostick et al. (2020a), show that a large portion of pyDOM can be respired (bio-degraded) without priming, which indicates that these pyrogenic molecules may be far less resistant to degradation than previously presumed.

The involvement of pyDOM within the global carbon cycle is complex, and in many cases poorly understood. There is a growing body of literature showing that significant amounts of pyOM are solubilized and exported to the global ocean (Dittmar et al., 2012; Jaffé et al., 2013; Wang et al., 2016; Marques et al., 2017; Jones et al., 2020). However, the estimated pyDOM production and seepage rates of 1440 $TgC \cdot y^{-1}$ (Bostick et al., 2018) are greater than previously reported riverine flux estimates (203 $Tg \cdot C \cdot y^{-1}$; Jaffé et al., 2013; rescaled by Bostick et al., 2018). In addition to the implied 86% loss of carbon during export, a recent study also reported that the stable carbon isotopic signature ($\delta^{13}C$) of oceanic ConAC are not terrigenous, but rather, marine-like (Wagner et al., 2019). This suggests that either all of the riverine-exported ConAC are being mineralized before reaching

https://doi.org/10.5194/bg-2021-23
Preprint. Discussion started: 12 May 2021

the global ocean or are chemically altered significantly to change its $\delta^{13}C$ isotopic signature (Jones et al., 2020). Furthermore, microbial and photochemical processes have been found to transform DOM with characteristic terrigenous DOM composition (compounds with lower H/C and higher O/C ratios) into compounds having characteristics of marine-derived DOM (compounds with higher H/C, lower O/C ratios; Rossel et al., 2013). Thus, pyDOM may simply be losing its diagnostic molecular and isotopic fingerprints during riverine export due to a variety of degradative post-production processes, as shown by the diversification observed in our study.

The cycling of organic matter in the environment has always been an enigma, and there has been a long-standing effort to explain the fate of land-derived DOM (terrigenous DOM including pyDOM) in the global ocean (Hedges et al., 1997). In a previous manuscript evaluating the photochemical transformation of pyDOM (Goranov et al., 2020), we suggested that biotic consumption of photo-degradation products of pyDOM ("small aliphatic compounds") could result in the formation of marine-like DOM. This hypothesis was tested by comparing our incubation products (the bio-produced formulas) to FT-ICR-MS formulas of several marine DOM samples (reported in Sect. 5 of the Supplement). An insignificant number of CRAM-like marine formulas (Hertkorn et al., 2006) was observed in these comparisons (4 – 272 common formulas, 0 – 6% overlap) contrasting with this proposition and suggesting that biotic incubations of photo-degraded pyDOM do not produce significant numbers of marine-like molecules.

An alternative idea is that the bio-produced molecules observed in this study are part of the fast-cycling, labile DOM pool per Hansell's model (Hansell and Carlson, 2015), and are quickly depleted in the natural environment. This parallels the findings of a recently published study (Hach et al., 2020) observing that microbially produced molecules are extremely labile and are, within hours, broken down and recombined with ambient DOM molecules. The closed laboratory systems in our study, may have enabled the observation of these highly labile molecules, whereas in the natural environment, they would have been quickly transformed, diluted, or mineralized to inorganic carbon resulting in their removal from analytical detection. The richness in nitrogen and peptide-like character of these new molecules suggest greater potential lability (Hach et al., 2020), and it is likely that the by-products of biotic degradation of pyDOM are readily incorporated into microbial food webs. This is consistent with the idea that terrigenous DOM is either mineralized to CO_2 or incorporated into food webs (Berggren et al., 2010a; Ward et al., 2013; Fasching et al., 2014). It is also consistent with the fact that the majority of organic nitrogen in the oceans is derived from microbial peptidoglycans (McCarthy et al., 1997, 1998; Simpson et al., 2011), and with observations of nitrogen from peptidoglycans in soil and sedimentary porewater systems (Schulten and Schnitzer, 1998; Hu et al., 2018, 2020).

The production of these highly variable and diverse molecules, compositionally, is likely a contributing factor to the large complexity of natural organic matter (Hertkorn et al., 2007; Hawkes et al., 2018). They contribute to the highly variable microbial exometabolomes observed previously (Antón et al., 2013; Watrous et al., 2013; Romano et al., 2014) and stimulate further questions about their function and fate within the global carbon cycle. In this study, we have used soil microbes, as the corresponding degradation by-products can be observed in both soil, groundwater, and partially in the upstream of rivers. Therefore, it would be critical to perform further studies with different microbial consortia (riverine, estuarine, marine, etc.) to fully understand the biological degradation of pyDOM in different environments.

5 Conclusions

This study probing the molecular changes occurring after biotic degradation of pyDOM revealed that soil microbes can effectively recycle and transform a significant portion of pyDOM molecules into labile microbial biomass. After the 10-day incubations, it appears that a wide range of molecules, both aromatic and aliphatic, were degraded, forming a highly diverse pool of compounds, including N-containing compounds with proteinaceous signatures and a peptidoglycan-like backbone. These observations are consistent with the previous identification of nitrogen from peptidoglycans in soils and oceans. These bio-produced compounds were highly specific for each pyDOM sample (very few common bio-produced molecular formulas among samples). The observed molecular labilization and diversification have implications for the studies of wildfire biogeochemistry, as this shows that microbial reworking of pyDOM can contribute to the large complexity and variability of natural

organic matter. This study reveals that 1) pyDOM can be a medium for microbial growth, and 2) previously considered "recalcitrant" pyrogenic molecules can be incorporated into microbial food webs. This suggests that pyDOM is a much more active component in the global carbon and nitrogen cycles, and future studies need to further evaluate the bio-reactivity of pyDOM with microbial consortia of different environments, as well as in the context of wetted soils, groundwater processes, cycling within the riverine and marine water columns, and other aspects of the global carbon and nitrogen cycles.

Data Availability. Research Data associated with this article can be accessed at https://doi.org/10.17632/kjkhy3tfys.1

Competing Interests. The authors declare that they have no conflict of interest.

Author Contributions. Conceptualization, A.I.G, A.S.W., K.W.B., A.R.Z., S.M., P.G.H.; Investigation, K.W.B., A.I.G.; Formal analysis, A.I.G.; Writing – Original Draft Preparation, A.I.G.; Writing – Review & Editing, A.I.G, A.S.W., K.W.B., A.R.Z., S.M., P.G.H.; Funding Acquisition, A.S.W., A.R.Z., S.M., P.G.H.

Acknowledgments. We thank Rachel L. Sleighter for providing the marine FT-ICR-MS data. We also thank Isaiah Ruhl, Dr. Deepti Varma, and Dr. Ravi Garimella for assistance during instrumental analyses at the COSMIC facility (Old Dominion University), and Dow Van Arnam (University of Florida) for design and construction of the biochar pyrolyzer and solar simulator. This project was funded by National Science Foundation (Geobiology and Low-Temperature Geochemistry Program, proposal numbers EAR-1451452 and EAR-1451367) and the Frank Batten Endowment Fund to Dr. Patrick G. Hatcher (Old Dominion University). Additionally, we appreciate Old Dominion University for supporting Aleksandar I. Goranov through the Dominion Fellowship. Lastly, we would like to express our gratitude to the editor and reviewers for their time and feedback in improving this manuscript.

References

Abboudi, M., Jeffrey, W. H., Ghiglione, J. F., Pujo-Pay, M., Oriol, L., Sempéré, R., Charrière, B., and Joux, F.: Effects of photochemical transformations of dissolved organic matter on bacterial metabolism and diversity in three contrasting coastal sites in the Northwestern Mediterranean Sea during summer, Microbial Ecology, 55, 344-357, https://doi.org/10.1007/s00248-007-9280-8, 2008.

Abiven, S., Hengartner, P., Schneider, M. P. W., Singh, N., and Schmidt, M. W. I.: Pyrogenic carbon soluble fraction is larger and more aromatic in aged charcoal than in fresh charcoal, Soil Biology & Biochemistry, 43, 1615-1617, https://doi.org/10.1016/j.soilbio.2011.03.027, 2011.

Antón, J., Lucio, M., Peña, A., Cifuentes, A., Brito-Echeverría, J., Moritz, F., Tziotis, D., López, C., Urdiain, M., Schmitt-Kopplin, P., and Rosselló-Móra, R.: High metabolomic microdiversity within co-occurring isolates of the extremely halophilic bacterium *Salinibacter ruber*, PLoS ONE, 8, 1-14, https://doi.org/10.1371/journal.pone.0064701, 2013.

Antony, R., Sanyal, A., Kapse, N., Dhakephalkar, P. K., Thamban, M., and Nair, S.: Microbial communities associated with Antarctic snow pack and their biogeochemical implications, Microbiological Research, 192, 192-202, https://doi.org/10.1016/j.micres.2016.07.004, 2016.

Antony, R., Willoughby, A. S., Grannas, A. M., Catanzano, V., Sleighter, R. L., Thamban, M., Hatcher, P. G., and Nair, S.: Molecular insights on dissolved organic matter transformation by supraglacial microbial communities, Environmental Science & Technology, 51, 4328-4337, https://doi.org/10.1021/acs.est.6b05780, 2017.

Antony, R., Willoughby, A. S., Grannas, A. M., Catanzano, V., Sleighter, R. L., Thamban, M., and Hatcher, P. G.: Photo-biochemical transformation of dissolved organic matter on the surface of the coastal East Antarctic ice sheet, Biogeochemistry, 141, 229-247, https://doi.org/10.1007/s10533-018-0516-0, 2018.

https://doi.org/10.5194/bg-2021-23
Preprint. Discussion started: 12 May 2021

Ascough, P. L., Bird, M. I., Francis, S. M., Thornton, B., Midwood, A. J., Scott, A. C., and Apperley, D.: Variability in oxidative degradation of charcoal: Influence of production conditions and environmental exposure, Geochimica et Cosmochimica Acta, 75, 2361-2378, https://doi.org/10.1016/j.gca.2011.02.002, 2011.

Bao, H., Niggemann, J., Luo, L., Dittmar, T., and Kao, S.-J.: Aerosols as a source of dissolved black carbon to the ocean, Nature Communications, 8, 1-7, https://doi.org/10.1038/s41467-017-00437-3, 2017.

Bax, A., and Davis, D. G.: MLEV-17-based two-dimensional homonuclear magnetization transfer spectroscopy, Journal of Magnetic Resonance, 65, 355-360, https://doi.org/10.1016/0022-2364(85)90018-6, 1985.

Benner, R., and Biddanda, B.: Photochemical transformations of surface and deep marine dissolved organic matter: Effects on bacterial growth, Limnology and Oceanography, 43, 1373-1378, https://doi.org/10.4319/lo.1998.43.6.1373, 1998.

Berggren, M., Laudon, H., Haei, M., Ström, L., and Jansson, M.: Efficient aquatic bacterial metabolism of dissolved low-molecular-weight compounds from terrestrial sources, The ISME Journal, 4, 408-416, https://doi.org/10.1038/ismej.2009.120, 2010a.

Berggren, M., Ström, L., Laudon, H., Karlsson, J., Jonsson, A., Giesler, R., Bergström, A.-K., and Jansson, M.: Lake secondary production fueled by rapid transfer of low molecular weight organic carbon from terrestrial sources to aquatic consumers, Ecology Letters, 13, 870-880, https://doi.org/10.1111/j.1461-0248.2010.01483.x, 2010b.

Bianchi, T. S.: The role of terrestrially derived organic carbon in the coastal ocean: A changing paradigm and the priming effect, Proceedings of the National Academy of Sciences of the United States of America, 108, 19473–19481, https://doi.org/10.1073/pnas.1017982108, 2011.

Billen, G., Servais, P., and Becquevort, S.: Dynamics of bacterioplankton in oligotrophic and eutrophic aquatic environments: Bottom-up or top-down control?, Hydrobiologia, 207, 37-42, https://doi.org/10.1007/BF00041438, 1990.

Bostick, K. W., Zimmerman, A. R., Wozniak, A. S., Mitra, S., and Hatcher, P. G.: Production and composition of pyrogenic dissolved organic matter from a logical series of laboratory-generated chars, Frontiers in Earth Science, 6, 1-14, https://doi.org/10.3389/feart.2018.00043, 2018.

Bostick, K. W., Zimmerman, A. R., Goranov, A. I., Mitra, S., Hatcher, P. G., and Wozniak, A. S.: Biolability of fresh and photodegraded pyrogenic dissolved organic matter from laboratory-prepared chars, ESSOAr [pre-print], https://doi.org/10.1002/essoar.10503766.1, 31 July 2020.

Bostick, K. W., Zimmerman, A. R., Goranov, A. I., Mitra, S., Hatcher, P. G., and Wozniak, A. S.: Photolability of pyrogenic dissolved organic matter from a thermal series of laboratory-prepared chars, Science of The Total Environment, 724, 1-9, https://doi.org/10.1016/j.scitotenv.2020.138198, 2020b.

Burns, R. G., DeForest, J. L., Marxsen, J., Sinsabaugh, R. L., Stromberger, M. E., Wallenstein, M. D., Weintraub, M. N., and Zoppini, A.: Soil enzymes in a changing environment: Current knowledge and future directions, Soil Biology & Biochemistry, 58, 216-234, https://doi.org/10.1016/j.soilbio.2012.11.009, 2013.

Chen, M., and Jaffé, R.: Photo- and bio-reactivity patterns of dissolved organic matter from biomass and soil leachates and surface waters in a subtropical wetland, Water Research, 61, 181-190, https://doi.org/10.1016/j.watres.2014.03.075, 2014.

Chistoserdova, L., Chen, S.-W., Lapidus, A., and Lidstrom, M. E.: Methylotrophy in *Methylobacterium extorquens* AM1 from a genomic point of view, Journal of Bacteriology, 185, 2980-2987, https://doi.org/10.1128/JB.185.10.2980-2987.2003, 2003.

Chistoserdova, L., and Kalyuzhnaya, M. G.: Current trends in methylotrophy, Trends in Microbiology, 26, 703-714, https://doi.org/10.1016/j.tim.2018.01.011, 2018.

Coble, P. G.: Characterization of marine and terrestrial DOM in seawater using excitation-emission matrix spectroscopy, Marine Chemistry, 51, 325-346, https://doi.org/10.1016/0304-4203(95)00062-3, 1996.

Coble, P. G., Lead, J., Baker, A., Reynolds, D. M., and Spencer, R. G. M.: Aquatic Organic Matter Fluorescence, Cambridge University Press, New York, NY, 2014.

912 Coppola, A. I., Seidel, M., Ward, N. D., Viviroli, D., Nascimento, G. S., Haghipour, N., Revels, B. N., Abiven,
913 S., Jones, M. W., Richey, J. E., Eglinton, T. I., Dittmar, T., and Schmidt, M. W. I.: Marked isotopic
914 variability within and between the Amazon River and marine dissolved black carbon pools, Nature
915 Communications, 10, 1-8, https://doi.org/10.1038/s41467-019-11543-9, 2019.
916 D'Andrilli, J., Fischer, S. J., and Rosario-Ortiz, F. L.: Advancing critical applications of high resolution mass
917 spectrometry for DOM assessments: Re-engaging with mass spectral principles, limitations, and data
918 analysis, Environmental Science & Technology, 54, 11654-11656,
919 https://doi.org/10.1021/acs.est.0c04557, 2020.
920 Dittmar, T., Koch, B., Hertkorn, N., and Kattner, G.: A simple and efficient method for the solid-phase extraction
921 of dissolved organic matter (SPE-DOM) from seawater, Limnology and Oceanography: Methods, 6, 230-
922 235, https://doi.org/10.4319/lom.2008.6.230, 2008.
923 Dittmar, T., and Paeng, J.: A heat-induced molecular signature in marine dissolved organic matter, Nature
924 Geoscience, 2, 175-179, https://doi.org/10.1038/ngeo440, 2009.
925 Dittmar, T., de Rezende, C. E., Manecki, M., Niggemann, J., Coelho Ovalle, A. R., Stubbins, A., and Bernardes,
926 M. C.: Continuous flux of dissolved black carbon from a vanished tropical forest biome, Nature
927 Geoscience, 5, 618-622, https://doi.org/10.1038/ngeo1541, 2012.
928 Druffel, E.: Comments on the importance of black carbon in the global carbon cycle, Marine Chemistry, 92, 197-
929 200, https://doi.org/10.1016/j.marchem.2004.06.026, 2004.
930 Dyrda, G., Boniewska-Bernacka, E., Man, D., Barchiewicz, K., and Słota, R.: The effect of organic solvents on
931 selected microorganisms and model liposome membrane, Molecular Biology Reports, 46, 3225-3232,
932 https://doi.org/10.1007/s11033-019-04782-y, 2019.
933 Fasching, C., Behounek, B., Singer, G. A., and Battin, T. J.: Microbial degradation of terrigenous dissolved
934 organic matter and potential consequences for carbon cycling in brown-water streams, Scientific Reports,
935 4, 1-7, https://doi.org/10.1038/srep04981, 2014.
936 Fitch, A., Orland, C., Willer, D., Emilson, E. J. S., and Tanentzap, A. J.: Feasting on terrestrial organic matter:
937 Dining in a dark lake changes microbial decomposition, Global change biology, 24, 5110-5122,
938 https://doi.org/10.1111/gcb.14391, 2018.
939 Fu, H. Y., Liu, H. T., Mao, J. D., Chu, W. Y., Li, Q. L., Alvarez, P. J. J., Qu, X. L., and Zhu, D. Q.: Photochemistry
940 of dissolved black carbon released from biochar: Reactive oxygen species generation and
941 phototransformation, Environmental Science & Technology, 50, 1218-1226,
942 https://doi.org/10.1021/acs.est.5b04314, 2016.
943 Fuchs, G., Boll, M., and Heider, J.: Microbial degradation of aromatic compounds - from one strategy to four,
944 Nature Reviews Microbiology, 9, 803-816, https://doi.org/10.1038/nrmicro2652, 2011.
945 Goldberg, E. D.: Black carbon in the environment: Properties and distribution, J. Wiley, New York, NY, 1985.
946 Gonsior, M., Hertkorn, N., Hinman, N., Dvorski, S. E., Harir, M., Cooper, W. J., and Schmitt-Kopplin, P.:
947 Yellowstone hot springs are organic chemodiversity hot spots, Scientific Reports, 8, 1-13,
948 https://doi.org/10.1038/s41598-018-32593-x, 2018.
949 Goranov, A. I., Wozniak, A. S., Bostick, K. W., Zimmerman, A. R., Mitra, S., and Hatcher, P. G.: Photochemistry
950 after fire: Structural transformations of pyrogenic dissolved organic matter elucidated by advanced
951 analytical techniques, Geochimica et Cosmochimica Acta, 290, 271-292,
952 https://doi.org/10.1016/j.gca.2020.08.030, 2020.
953 Gottlieb, H. E., Kotlyar, V., and Nudelman, A.: NMR chemical shifts of common laboratory solvents as trace
954 impurities, The Journal of Organic Chemistry, 62, 7512-7515, https://doi.org/10.1021/Jo971176v, 1997.
955 Green, S. A., and Blough, N. V.: Optical absorption and fluorescence properties of chromophoric dissolved
956 organic matter in natural waters, Limnology and Oceanography, 39, 1903-1916,
957 https://doi.org/10.4319/lo.1994.39.8.1903, 1994.
958 Guenet, B., Danger, M., Abbadie, L., and Lacroix, G.: Priming effect: Bridging the gap between terrestrial and
959 aquatic ecology, Ecology, 91, 2850-2861, https://doi.org/10.1890/09-1968.1, 2010.

960 Gurganus, S. C., Wozniak, A. S., and Hatcher, P. G.: Molecular characteristics of the water soluble organic matter
961 in size-fractionated aerosols collected over the North Atlantic Ocean, Marine Chemistry, 170, 37-48,
962 https://doi.org/10.1016/j.marchem.2015.01.007, 2015.
963 Hach, P. F., Marchant, H. K., Krupke, A., Riedel, T., Meier, D. V., Lavik, G., Holtappels, M., Dittmar, T., and
964 Kuypers, M. M. M.: Rapid microbial diversification of dissolved organic matter in oceanic surface waters
965 leads to carbon sequestration, Scientific Reports, 10, 1-10, https://doi.org/10.1038/s41598-020-69930-y,
966 2020.
967 Hansell, D. A., and Carlson, C. A.: Biogeochemistry of marine dissolved organic matter, Second ed., Academic
968 Press, Amsterdam, 712 pp., 2015.
969 Hawkes, J. A., Patriarca, C., Sjöberg, P. J. R., Tranvik, L. J., and Bergquist, J.: Extreme isomeric complexity of
970 dissolved organic matter found across aquatic environments, Limnology and Oceanography Letters, 3,
971 21-30, https://doi.org/10.1002/lol2.10064, 2018.
972 Hedges, J. I., Keil, R. G., and Benner, R.: What happens to terrestrial organic matter in the ocean?, Organic
973 Geochemistry, 27, 195-212, https://doi.org/10.1016/S0146-6380(97)00066-1, 1997.
974 Helms, J. R., Stubbins, A., Ritchie, J. D., Minor, E. C., Kieber, D. J., and Mopper, K.: Absorption spectral slopes
975 and slope ratios as indicators of molecular weight, source, and photobleaching of chromophoric dissolved
976 organic matter, Limnology and Oceanography, 53, 955-969, https://doi.org/10.4319/lo.2008.53.3.0955,
977 2008.
978 Hemmler, D., Gonsior, M., Powers, L. C., Marshall, J. W., Rychlik, M., Taylor, A. J., and Schmitt-Kopplin, P.:
979 Simulated sunlight selectively modifies Maillard reaction products in a wide array of chemical reactions,
980 Chemistry, 25, 13208-13217, https://doi.org/10.1002/chem.201902804, 2019.
981 Hertkorn, N., Benner, R., Frommberger, M., Schmitt-Kopplin, P., Witt, M., Kaiser, K., Kettrup, A., and Hedges,
982 J. I.: Characterization of a major refractory component of marine dissolved organic matter, Geochimica
983 et Cosmochimica Acta, 70, 2990-3010, https://doi.org/10.1016/j.gca.2006.03.021, 2006.
984 Hertkorn, N., Ruecker, C., Meringer, M., Gugisch, R., Frommberger, M., Perdue, E., Witt, M., and Schmitt-
985 Kopplin, P.: High-precision frequency measurements: Indispensable tools at the core of the molecular-
986 level analysis of complex systems, Analytical and Bioanalytical Chemistry, 389, 1311-1327,
987 https://doi.org/10.1007/s00216-007-1577-4, 2007.
988 Higuchi, T.: Microbial degradation of lignin: Role of lignin peroxidase, manganese peroxidase, and laccase,
989 Proceedings of the Japan Academy, Series B, 80, 204-214, https://doi.org/10.2183/pjab.80.204, 2004.
990 Hockaday, W. C., Grannas, A. M., Kim, S., and Hatcher, P. G.: Direct molecular evidence for the degradation
991 and mobility of black carbon in soils from ultrahigh-resolution mass spectral analysis of dissolved organic
992 matter from a fire-impacted forest soil, Organic Geochemistry, 37, 501-510,
993 https://doi.org/10.1016/j.orggeochem.2005.11.003, 2006.
994 Hockaday, W. C., Grannas, A. M., Kim, S., and Hatcher, P. G.: The transformation and mobility of charcoal in a
995 fire-impacted watershed, Geochimica et Cosmochimica Acta, 71, 3432-3445,
996 https://doi.org/10.1016/j.gca.2007.02.023, 2007.
997 Hu, Y., Zheng, Q., Zhang, S., Noll, L., and Wanek, W.: Significant release and microbial utilization of amino
998 sugars and D-amino acid enantiomers from microbial cell wall decomposition in soils, Soil Biology &
999 Biochemistry, 123, 115-125, https://doi.org/10.1016/j.soilbio.2018.04.024, 2018.
.000 Hu, Y., Zheng, Q., Noll, L., Zhang, S., and Wanek, W.: Direct measurement of the *in situ* decomposition of
.001 microbial-derived soil organic matter, Soil Biology & Biochemistry, 141, 1-10,
.002 https://doi.org/10.1016/j.soilbio.2019.107660, 2020.
.003 Hughey, C. A., Hendrickson, C. L., Rodgers, R. P., Marshall, A. G., and Qian, K.: Kendrick mass defect spectrum:
.004 a compact visual analysis for ultrahigh-resolution broadband mass spectra, Analytical Chemistry, 73,
.005 4676-4681, https://doi.org/10.1021/ac010560w, 2001.
.006 Hyde, S. M., and Wood, P. M.: A mechanism for production of hydroxyl radicals by the brown-rot fungus
.007 *Coniophora Puteana*: Fe(III) reduction by cellobiose dehydrogenase and Fe(II) oxidation at a distance
.008 from the hyphae, Microbiology, 143, 259-266, https://doi.org/10.1099/00221287-143-1-259, 1997.

Idowu, O., Semple, K. T., Ramadass, K., O'Connor, W., Hansbro, P., and Thavamani, P.: Beyond the obvious: Environmental health implications of polar polycyclic aromatic hydrocarbons, Environ Int, 123, 543-557, https://doi.org/10.1016/j.envint.2018.12.051, 2019.

Jaffé, R., Ding, Y., Niggemann, J., Vähätalo, A. V., Stubbins, A., Spencer, R. G. M., Campbell, J., and Dittmar, T.: Global charcoal mobilization from soils via dissolution and riverine transport to the oceans, Science, 340, 345-347, https://doi.org/10.1126/science.1231476, 2013.

Johns, G: Austin Cary Forest Prescribed Burn (33/8S/21E), School of Forest Resources and Conservation, UF/IFAS, Prescribed Burn Prescription 721, 1-5, 2016

Jones, M. W., Coppola, A. I., Santín, C., Dittmar, T., Jaffé, R., Doerr, S. H., and Quine, T. A.: Fires prime terrestrial organic carbon for riverine export to the global oceans, Nature Communications, 11, 1-8, https://doi.org/10.1038/s41467-020-16576-z, 2020.

Judd, K. E., Crump, B. C., and Kling, G. W.: Bacterial responses in activity and community composition to photo-oxidation of dissolved organic matter from soil and surface waters, Aquatic Sciences, 69, 96-107, https://doi.org/10.1007/s00027-006-0908-4, 2007.

Kendrick, E.: A mass scale based on CH_2 = 14.0000 for high resolution mass spectrometry of organic compounds, Analytical Chemistry, 35, 2146-2154, https://doi.org/10.1021/ac60206a048, 1963.

Khatami, S., Deng, Y., Tien, M., and Hatcher, P. G.: Formation of water-soluble organic matter through fungal degradation of lignin, Organic Geochemistry, 135, 64-70, https://doi.org/10.1016/j.orggeochem.2019.06.004, 2019a.

Khatami, S., Deng, Y., Tien, M., and Hatcher, P. G.: Lignin contribution to aliphatic constituents of humic acids through fungal degradation, Journal of Environmental Quality, 48, 1565-1570, https://doi.org/10.2134/jeq2019.01.0034, 2019b.

Khodadad, C. L. M., Zimmerman, A. R., Green, S. J., Uthandi, S., and Foster, J. S.: Taxa-specific changes in soil microbial community composition induced by pyrogenic carbon amendments, Soil Biology & Biochemistry, 43, 385-392, https://doi.org/10.1016/j.soilbio.2010.11.005, 2011.

Kieber, D. J., McDaniel, J., and Mopper, K.: Photochemical source of biological substrates in sea water: Implications for carbon cycling, Nature, 341, 637-639, https://doi.org/10.1038/341637a0, 1989.

Kim, S., Kramer, R. W., and Hatcher, P. G.: Graphical method for analysis of ultrahigh-resolution broadband mass spectra of natural organic matter, the van Krevelen diagram, Analytical Chemistry, 75, 5336-5344, https://doi.org/10.1021/ac034415p, 2003.

Kirchman, D. L.: Processes in microbial ecology, Second ed., Oxford University Press, 1-318 pp., 2018.

Klevit, R. E.: Improving two-dimensional NMR spectra by t_1 ridge subtraction, Journal of Magnetic Resonance, 62, 551-555, https://doi.org/10.1016/0022-2364(85)90227-6, 1985.

Koch, B. P., and Dittmar, T.: From mass to structure: An aromaticity index for high-resolution mass data of natural organic matter, Rapid Communications in Mass Spectrometry, 20, 926-932, https://doi.org/10.1002/rcm.2386, 2006.

Koch, B. P., Dittmar, T., Witt, M., and Kattner, G.: Fundamentals of molecular formula assignment to ultrahigh resolution mass data of natural organic matter, Analytical Chemistry, 79, 1758-1763, https://doi.org/10.1021/ac061949s, 2007.

Koch, B. P., and Dittmar, T.: From mass to structure: An aromaticity index for high-resolution mass data of natural organic matter (Erratum), Rapid Communications in Mass Spectrometry, 30, 1, https://doi.org/10.1002/rcm.7433, 2016.

Kolb, S., and Stacheter, A.: Prerequisites for amplicon pyrosequencing of microbial methanol utilizers in the environment, Front Microbiol, 4, 1-12, https://doi.org/10.3389/fmicb.2013.00268, 2013.

Kothawala, D. N., Murphy, K. R., Stedmon, C. A., Weyhenmeyer, G. A., and Tranvik, L. J.: Inner filter correction of dissolved organic matter fluorescence, Limnology and Oceanography: Methods, 11, 616-630, https://doi.org/10.4319/lom.2013.11.616, 2013.

Kujawinski, E. B., and Behn, M. D.: Automated analysis of electrospray ionization Fourier transform ion cyclotron resonance mass spectra of natural organic matter, Analytical Chemistry, 78, 4363-4373, https://doi.org/10.1021/ac0600306, 2006.

Kuzyakov, Y., Subbotina, I., Chen, H., Bogomolova, I., and Xu, X.: Black carbon decomposition and incorporation into soil microbial biomass estimated by ^{14}C labeling, Soil Biology & Biochemistry, 41, 210-219, https://doi.org/10.1016/j.soilbio.2008.10.016, 2009.

Kuzyakov, Y., Bogomolova, I., and Glaser, B.: Biochar stability in soil: Decomposition during eight years and transformation as assessed by compound-specific ^{14}C analysis, Soil Biology & Biochemistry, 70, 229-236, https://doi.org/10.1016/j.soilbio.2013.12.021, 2014.

Lechtenfeld, O. J., Hertkorn, N., Shen, Y., Witt, M., and Benner, R.: Marine sequestration of carbon in bacterial metabolites, Nature Communications, 6, 1-8, https://doi.org/10.1038/ncomms7711, 2015.

Lehmann, J.: A handful of carbon, Nature, 447, 143-144, https://doi.org/10.1038/447143a, 2007.

Li, M., Bao, F., Zhang, Y., Sheng, H., Chen, C., and Zhao, J.: Photochemical aging of soot in the aqueous phase: Release of dissolved black carbon and the formation of $^1O_2$, Environmental Science & Technology, 53, 12311-12319, https://doi.org/10.1021/acs.est.9b02773, 2019.

Lindell, M. J., Granéli, W., and Tranvik, L. J.: Enhanced bacterial growth in response to photochemical transformation of dissolved organic matter, Limnology and Oceanography, 40, 195-199, https://doi.org/10.4319/lo.1995.40.1.0195, 1995.

Liu, M., Mao, X.-a., Ye, C., Huang, H., Nicholson, J. K., and Lindon, J. C.: Improved WATERGATE pulse sequences for solvent suppression in NMR spectroscopy, Journal of Magnetic Resonance, 132, 125-129, https://doi.org/10.1006/jmre.1998.1405, 1998.

Marques, J. S. J., Dittmar, T., Niggemann, J., Almeida, M. G., Gomez-Saez, G. V., and Rezende, C. E.: Dissolved black carbon in the headwaters-to-ocean continuum of Paraíba Do Sul River, Brazil, Frontiers in Earth Science, 5, 1-12, https://doi.org/10.3389/feart.2017.00011, 2017.

Masiello, C. A., and Druffel, E. R. M.: Black carbon in deep-sea sediments, Science, 280, 1911-1913, https://doi.org/10.1126/science.280.5371.1911, 1998.

Masiello, C. A.: New directions in black carbon organic geochemistry, Marine Chemistry, 92, 201-213, https://doi.org/10.1016/j.marchem.2004.06.043, 2004.

McCarthy, M., Pratum, T., Hedges, J., and Benner, R.: Chemical composition of dissolved organic nitrogen in the ocean, Nature, 390, 150-154, https://doi.org/10.1038/36535, 1997.

McCarthy, M. D., Hedges, J. I., and Benner, R.: Major bacterial contribution to marine dissolved organic nitrogen, Science, 281, 231-234, https://doi.org/10.1126/science.281.5374.231, 1998.

McKee, G. A., Kobiela, M. E., and Hatcher, P. G.: Effect of Michael adduction on peptide preservation in natural waters, Environmental Science: Processes & Impacts, 16, 2087-2097, 10.1039/C4EM00075G, 2014.

McNally, A. M., Moody, E. C., and McNeill, K.: Kinetics and mechanism of the sensitized photodegradation of lignin model compounds, Photochem. Photobiol. Sci., 4, 268-274, https://doi.org/10.1039/b416956e, 2005.

Miller, M. P., Simone, B. E., McKnight, D. M., Cory, R. M., Williams, M. W., and Boyer, E. W.: New light on a dark subject: Comment, Aquatic Sciences, 72, 269-275, https://doi.org/10.1007/s00027-010-0130-2, 2010.

Moran, M. A., and Covert, J. S.: Photochemically mediated linkages between dissolved organic matter and bacterioplankton, in: Aquatic Ecosystems, edited by: Findlay, S. E. G., and Sinsabaugh, R. L., Academic Press, Burlington, 243-262, 2003.

Moran, M. A., Kujawinski, E. B., Stubbins, A., Fatland, R., Aluwihare, L. I., Buchan, A., Crump, B. C., Dorrestein, P. C., Dyhrman, S. T., Hess, N. J., Howe, B., Longnecker, K., Medeiros, P. M., Niggemann, J., Obernosterer, I., Repeta, D. J., and Waldbauer, J. R.: Deciphering ocean carbon in a changing world, Proceedings of the National Academy of Sciences of the United States of America, 113, 3143-3151, 10.1073/pnas.1514645113, 2016.

Múčka, V., Bláha, P., Čuba, V., and Červenák, J.: Influence of various scavengers of •OH radicals on the radiation sensitivity of yeast and bacteria, International Journal of Radiation Biology, 89, 1045-1052, https://doi.org/10.3109/09553002.2013.817702, 2013.

Mukherjee, A., Zimmerman, A. R., and Harris, W.: Surface chemistry variations among a series of laboratory-produced biochars, Geoderma, 163, 247-255, https://doi.org/10.1016/j.geoderma.2011.04.021, 2011.

Mukherjee, A., and Zimmerman, A. R.: Organic carbon and nutrient release from a range of laboratory-produced biochars and biochar-soil mixtures, Geoderma, 193-194, 122-130, https://doi.org/10.1016/j.geoderma.2012.10.002, 2013.

Murphy, K. R., Butler, K. D., Spencer, R. G. M., Stedmon, C. A., Boehme, J. R., and Aiken, G. R.: Measurement of dissolved organic matter fluorescence in aquatic environments: An interlaboratory comparison, Environmental Science & Technology, 44, 9405-9412, https://doi.org/10.1021/es102362t, 2010.

Murphy, K. R.: A note on determining the extent of the water Raman peak in fluorescence spectroscopy, Applied Spectroscopy, 65, 233-236, https://doi.org/10.1366/10-06136, 2011.

Murphy, K. R., Stedmon, C. A., Graeber, D., and Bro, R.: Fluorescence spectroscopy and multi-way techniques. PARAFAC, Analytical Methods, 5, 6541-6882, https://doi.org/10.1039/c3ay41160e, 2013.

Nalven, S. G., Ward, C. P., Payet, J. P., Cory, R. M., Kling, G. W., Sharpton, T. J., Sullivan, C. M., and Crump, B. C.: Experimental metatranscriptomics reveals the costs and benefits of dissolved organic matter photo-alteration for freshwater microbes, Environmental Microbiology, 22, 3505-3521, https://doi.org/10.1111/1462-2920.15121, 2020.

Obernosterer, I., and Benner, R.: Competition between biological and photochemical processes in the mineralization of dissolved organic carbon, Limnology and Oceanography, 49, 117-124, https://doi.org/10.4319/lo.2004.49.1.0117, 2004.

Patriarca, C., Balderrama, A., Može, M., Sjöberg, P. J. R., Bergquist, J., Tranvik, L. J., and Hawkes, J. A.: Investigating the ionization of dissolved organic matter by electrospray ionization, Analytical Chemistry, 92, 14210-14218, https://doi.org/10.1021/acs.analchem.0c03438, 2020.

Porcal, P., Dillon, P. J., and Molot, L. A.: Photochemical production and decomposition of particulate organic carbon in a freshwater stream, Aquatic Sciences, 75, 469-482, https://doi.org/10.1007/s00027-013-0293-8, 2013.

Powers, L. C., Hertkorn, N., McDonald, N., Schmitt-Kopplin, P., Del Vecchio, R., Blough, N. V., and Gonsior, M.: *Sargassum sp.* act as a large regional surce of marine dissolved organic carbon and polyphenols, Global Biogeochemical Cycles, 33, 1423-1439, https://doi.org/10.1029/2019GB006225, 2019.

Qi, Y., Fu, W., Tian, J., Luo, C., Shan, S., Sun, S., Ren, P., Zhang, H., Liu, J., Zhang, X., and Wang, X.: Dissolved black carbon is not likely a significant refractory organic carbon pool in rivers and oceans, Nature Communications, 11, 1-11, https://doi.org/10.1038/s41467-020-18808-8, 2020.

Qualls, R. G., and Richardson, C. J.: Factors controlling concentration, export, and decomposition of dissolved organic nutrients in the Everglades of Florida, Biogeochemistry, 62, 197-229, https://doi.org/10.1023/A:1021150503664, 2003.

Quan, G., Fan, Q., Zimmerman, A. R., Sun, J., Cui, L., Wang, H., Gao, B., and Yan, J.: Effects of laboratory biotic aging on the characteristics of biochar and its water-soluble organic products, Journal of Hazardous Materials, 382, 1-9, https://doi.org/10.1016/j.jhazmat.2019.121071, 2020.

Reisser, M., Purves, R. S., Schmidt, M. W. I., and Abiven, S.: Pyrogenic carbon in soils: A literature-based inventory and a global estimation of its content in soil organic carbon and stocks, Frontiers in Earth Science, 4, 1-14, https://doi.org/10.3389/feart.2016.00080, 2016.

Riedel, T., Zark, M., Vähätalo, A. V., Niggemann, J., Spencer, R. G. M., Hernes, P. J., and Dittmar, T.: Molecular signatures of biogeochemical transformations in dissolved organic matter from ten world rivers, Frontiers in Earth Science, 4, 1-16, https://doi.org/10.3389/feart.2016.00085, 2016.

Roebuck, J. A., Podgorksi, D. C., Wagner, S., and Jaffé, R.: Photodissolution of charcoal and fire-impacted soil as a potential source of dissolved black carbon in aquatic environments, Organic Geochemistry, 112, 16-21, https://doi.org/10.1016/j.orggeochem.2017.06.018, 2017.

Romano, S., Dittmar, T., Bondarev, V., Weber, R. J. M., Viant, M. R., and Schulz-Vogt, H. N.: Exo-metabolome of *Pseudovibrio sp.* FO-BEG1 analyzed by ultra-high resolution mass spectrometry and the effect of phosphate limitation, PLoS ONE, 9, 1-11, https://doi.org/10.1371/journal.pone.0096038, 2014.

Rossel, P. E., Vähätalo, A. V., Witt, M., and Dittmar, T.: Molecular composition of dissolved organic matter from a wetland plant (*Juncus effusus*) after photochemical and microbial decomposition (1.25 yr): Common

features with deep sea dissolved organic matter, Organic Geochemistry, 60, 62-71, https://doi.org/10.1016/j.orggeochem.2013.04.013, 2013.
Santín, C., Doerr, S. H., Preston, C. M., and Gonzalez-Rodriguez, G.: Pyrogenic organic matter production from wildfires: A missing sink in the global carbon cycle, Global change biology, 21, 1621-1633, https://doi.org/10.1111/gcb.12800, 2015.
Santín, C., Doerr, S. H., Merino, A., Bryant, R., and Loader, N. J.: Forest floor chemical transformations in a boreal forest fire and their correlations with temperature and heating duration, Geoderma, 264, 71-80, https://doi.org/10.1016/j.geoderma.2015.09.021, 2016.
Santín, C., Doerr, S. H., Merino, A., Bucheli, T. D., Bryant, R., Ascough, P., Gao, X., and Masiello, C. A.: Carbon sequestration potential and physicochemical properties differ between wildfire charcoals and slow-pyrolysis biochars, Scientific Reports, 7, 1-11, https://doi.org/10.1038/s41598-017-10455-2, 2017.
Schmidt, M. W. I., and Noack, A. G.: Black carbon in soils and sediments: Analysis, distribution, implications, and current challenges, Global Biogeochemical Cycles, 14, 777-793, https://doi.org/10.1029/1999GB001208, 2000.
Schneider, M. P. W., Hilf, M., Vogt, U. F., and Schmidt, M. W. I.: The benzene polycarboxylic acid (BPCA) pattern of wood pyrolyzed between 200 ^{O}C and 1000 ^{O}C, Organic Geochemistry, 41, 1082-1088, https://doi.org/10.1016/j.orggeochem.2010.07.001, 2010.
Schulten, H. R., and Schnitzer, M.: The chemistry of soil organic nitrogen: A review, Biology and fertility of soils, 26, 1-15, https://doi.org/10.1007/s003740050335, 1998.
Scully, N. M., Cooper, W. J., and Tranvik, L. J.: Photochemical effects on microbial activity in natural waters: The interaction of reactive oxygen species and dissolved organic matter, FEMS Microbiology Ecology, 46, 353-357, https://doi.org/10.1016/s0168-6496(03)00198-3, 2003.
Simpson, A. J., McNally, D. J., and Simpson, M. J.: NMR spectroscopy in environmental research: From molecular interactions to global processes, Progress in Nuclear Magnetic Resonance Spectroscopy, 58, 97-175, https://doi.org/10.1016/j.pnmrs.2010.09.001, 2011.
Sinsabaugh, R. L., Findlay, S., Franchini, P., and Fischer, D.: Enzymatic analysis of riverine bacterioplankton production, Limnology and Oceanography, 42, 29-38, https://doi.org/10.4319/lo.1997.42.1.0029, 1997.
Skjemstad, J., Reicosky, D. C., Wilts, A., and McGowan, J.: Charcoal carbon in U.S. agricultural soils, Soil Science Society of America Journal, 66, 1249-1255, https://doi.org/10.2136/sssaj2002.1249, 2002.
Sleighter, R. L., McKee, G. A., Liu, Z., and Hatcher, P. G.: Naturally present fatty acids as internal calibrants for Fourier transform mass spectra of dissolved organic matter, Limnology and Oceanography: Methods, 6, 246-253, https://doi.org/10.4319/lom.2008.6.246, 2008.
Sleighter, R. L., Chen, H., Wozniak, A. S., Willoughby, A. S., Caricasole, P., and Hatcher, P. G.: Establishing a measure of reproducibility of ultrahigh-resolution mass spectra for complex mixtures of natural organic matter, Analytical Chemistry, 84, 9184-9191, https://doi.org/10.1021/ac3018026, 2012.
Smith, C. R., Hatcher, P. G., Kumar, S., and Lee, J. W.: Investigation into the sources of biochar water-soluble organic compounds and their potential toxicity on aquatic microorganisms, ACS Sustainable Chemistry & Engineering, 4, 2550-2558, https://doi.org/10.1021/acssuschemeng.5b01687, 2016.
Søndergaard, M., and Middelboe, M.: A cross-system analysis of labile dissolved organic carbon, Marine Ecology Progress Series, 118, 283-294, https://doi.org/10.3354/meps118283, 1995.
Spence, A., Simpson, A. J., McNally, D. J., Moran, B. W., McCaul, M. V., Hart, K., Paull, B., and Kelleher, B. P.: The degradation characteristics of microbial biomass in soil, Geochimica et Cosmochimica Acta, 75, 2571-2581, https://doi.org/10.1016/j.gca.2011.03.012, 2011.
Stenson, A. C., William, M., Marshall, A. G., and Cooper, W. T.: Ionization and fragmentation of humic substances in electrospray ionization Fourier transform-ion cyclotron resonance mass spectrometry, Analytical Chemistry, 74, 4397-4409, 2002.
Stubbins, A., Spencer, R. G. M., Chen, H. M., Hatcher, P. G., Mopper, K., Hernes, P. J., Mwamba, V. L., Mangangu, A. M., Wabakanghanzi, J. N., and Six, J.: Illuminated darkness: Molecular signatures of Congo River dissolved organic matter and its photochemical alteration as revealed by ultrahigh precision mass spectrometry, Limnology and Oceanography, 55, 1467-1477, 10.4319/lo.2010.55.4.1467, 2010.

https://doi.org/10.5194/bg-2021-23
Preprint. Discussion started: 12 May 2021

Stubbins, A., Niggemann, J., and Dittmar, T.: Photo-lability of deep ocean dissolved black carbon, Biogeosciences, 9, 1661-1670, https://doi.org/10.5194/bg-9-1661-2012, 2012.
Sun, L., Xu, C., Zhang, S., Lin, P., Schwehr, K. A., Quigg, A., Chiu, M.-H., Chin, W.-C., and Santschi, P. H.: Light-induced aggregation of microbial exopolymeric substances, Chemosphere, 181, 675-681, https://doi.org/10.1016/j.chemosphere.2017.04.099, 2017.
Trusiak, A., Treibergs, L., Kling, G., and Cory, R.: The controls of iron and oxygen on hydroxyl radical (•OH) production in soils, Soil Systems, 3, 1-23, https://doi.org/10.3390/soilsystems3010001, 2018.
Valle, J., Harir, M., Gonsior, M., Enrich-Prast, A., Schmitt-Kopplin, P., Bastviken, D., and Hertkorn, N.: Molecular differences between water column and sediment pore water SPE-DOM in ten Swedish boreal lakes, Water Research, 170, 1-11, https://doi.org/10.1016/j.watres.2019.115320, 2020.
Van Krevelen, D. W.: Graphical-statistical method for the study of structure and reaction processes of coal, Fuel Processing Technology, 29, 269-228, 1950.
Vollmer, W., Blanot, D., and De Pedro, M. A.: Peptidoglycan structure and architecture, FEMS Microbiology Reviews, 32, 149-167, https://doi.org/10.1111/j.1574-6976.2007.00094.x, 2008.
Vorobev, A., Sharma, S., Yu, M., Lee, J., Washington, B. J., Whitman, W. B., Ballantyne, F. t., Medeiros, P. M., and Moran, M. A.: Identifying labile DOM components in a coastal ocean through depleted bacterial transcripts and chemical signals, Environmental Microbiology, 20, 3012-3030, https://doi.org/10.1111/1462-2920.14344, 2018.
Waggoner, D. C., Chen, H., Willoughby, A. S., and Hatcher, P. G.: Formation of black carbon-like and alicyclic aliphatic compounds by hydroxyl radical initiated degradation of lignin, Organic Geochemistry, 82, 69-76, https://doi.org/10.1016/j.orggeochem.2015.02.007, 2015.
Waggoner, D. C., and Hatcher, P. G.: Hydroxyl radical alteration of HPLC fractionated lignin: Formation of new compounds from terrestrial organic matter, Organic Geochemistry, 113, 315-325, https://doi.org/10.1016/j.orggeochem.2017.07.011, 2017.
Waggoner, D. C., Wozniak, A. S., Cory, R. M., and Hatcher, P. G.: The role of reactive oxygen species in the degradation of lignin derived dissolved organic matter, Geochimica et Cosmochimica Acta, 208, 171-184, https://doi.org/10.1016/j.gca.2017.03.036, 2017.
Wagner, S., and Jaffé, R.: Effect of photodegradation on molecular size distribution and quality of dissolved black carbon, Organic Geochemistry, 86, 1-4, https://doi.org/10.1016/j.orggeochem.2015.05.005, 2015.
Wagner, S., Ding, Y., and Jaffé, R.: A new perspective on the apparent solubility of dissolved black carbon, Frontiers in Earth Science, 5, 1-16, https://doi.org/10.3389/feart.2017.00075, 2017.
Wagner, S., Jaffé, R., and Stubbins, A.: Dissolved black carbon in aquatic ecosystems, Limnology and Oceanography Letters, 3, 168-185, https://doi.org/10.1002/lol2.10076, 2018.
Wagner, S., Brandes, J., Spencer, R. G. M., Ma, K., Rosengard, S. Z., Moura, J. M. S., and Stubbins, A.: Isotopic composition of oceanic dissolved black carbon reveals non-riverine source, Nature Communications, 10, 1-8, https://doi.org/10.1038/s41467-019-13111-7, 2019.
Wang, H., Zhou, H., Ma, J., Nie, J., Yan, S., and Song, W.: Triplet photochemistry of dissolved black carbon and its effects on the photochemical formation of reactive oxygen species, Environmental Science & Technology, 54, 4903-4911, https://doi.org/10.1021/acs.est.0c00061, 2020.
Wang, X., Xu, C., Druffel, E. M., Xue, Y., and Qi, Y.: Two black carbon pools transported by the Changjiang and Huanghe Rivers in China, Global Biogeochemical Cycles, 30, 1778-1790, https://doi.org/10.1002/2016GB005509, 2016.
Ward, C. P., Sleighter, R. L., Hatcher, P. G., and Cory, R. M.: Insights into the complete and partial photooxidation of black carbon in surface waters, Environmental Science: Processes & Impacts, 16, 721-731, https://doi.org/10.1039/C3EM00597F, 2014.
Ward, N. D., Keil, R. G., Medeiros, P. M., Brito, D. C., Cunha, A. C., Dittmar, T., Yager, P. L., Krusche, A. V., and Richey, J. E.: Degradation of terrestrially derived macromolecules in the Amazon River, Nature Geoscience, 6, 530-533, https://doi.org/10.1038/ngeo1817, 2013.

https://doi.org/10.5194/bg-2021-23
Preprint. Discussion started: 12 May 2021

256 Watrous, J., Roach, P., Heath, B., Alexandrov, T., Laskin, J., and Dorrestein, P. C.: Metabolic profiling directly
257 from the Petri dish using nanospray desorption electrospray ionization imaging mass spectrometry,
258 Analytical Chemistry, 85, 10385-10391, https://doi.org/10.1021/ac4023154, 2013.
259 Weishaar, J. L., Aiken, G. R., Bergamaschi, B. A., Fram, M. S., Fujii, R., and Mopper, K.: Evaluation of specific
260 ultraviolet absorbance as an indicator of the chemical composition and reactivity of dissolved organic
261 carbon, Environmental Science & Technology, 37, 4702-4708, https://doi.org/10.1021/es030360x, 2003.
262 Wetzel, R. G., Hatcher, P. G., and Bianchi, T. S.: Natural photolysis by ultraviolet irradiance of recalcitrant
263 dissolved organic matter to simple substrates for rapidbacterial metabolism, Limnology and
264 Oceanography, 40, 1369-1380, https://doi.org/10.4319/lo.1995.40.8.1369, 1995.
265 Wienhausen, G., Noriega-Ortega, B. E., Niggemann, J., Dittmar, T., and Simon, M.: The exometabolome of two
266 model strains of the *Roseobacter* group: A marketplace of microbial metabolites, Front Microbiol, 8, 1-
267 15, https://doi.org/10.3389/fmicb.2017.01985, 2017.
268 Wozniak, A., Bauer, J., Sleighter, R., Dickhut, R., and Hatcher, P.: Technical note: Molecular characterization of
269 aerosol-derived water soluble organic carbon using ultrahigh resolution electrospray ionization Fourier
270 transform ion cyclotron resonance mass spectrometry, Atmospheric Chemistry and Physics, 8, 5099-5111,
271 https://doi.org/10.5194/acp-8-5099-2008, 2008.
272 Wozniak, A. S., Goranov, A. I., Mitra, S., Bostick, K. W., Zimmerman, A. R., Schlesinger, D. R., Myneni, S.,
273 and Hatcher, P. G.: Molecular heterogeneity in pyrogenic dissolved organic matter from a thermal series
274 of oak and grass chars, Organic Geochemistry, 148, 1-18,
275 https://doi.org/10.1016/j.orggeochem.2020.104065, 2020.
276 Wünsch, U. J., Bro, R., Stedmon, C. A., Wenig, P., and Murphy, K. R.: Emerging patterns in the global
277 distribution of dissolved organic matter fluorescence, Analytical Methods, 11, 888-893,
278 https://doi.org/10.1039/C8AY02422G, 2019.
279 Xiao, Y., Carena, L., Näsi, M.-T., and Vähätalo, A. V.: Superoxide-driven autocatalytic dark production of
280 hydroxyl radicals in the presence of complexes of natural dissolved organic matter and iron, Water
281 Research, 1-8, https://doi.org/10.1016/j.watres.2020.115782, 2020.
282 Yavitt, J. B., and Fahey, T. J.: An experimental analysis of solution chemistry in a lodgepole pine forest foor,
283 Oikos, 43, 222-234, https://doi.org/10.2307/3544772, 1984.
284 Zeng, Y., Hong, P. K. A., and Wavrek, D. A.: Chemical-biological treatment of pyrene, Water Research, 34,
285 1157-1172, https://doi.org/10.1016/S0043-1354(99)00270-5, 2000a.
286 Zeng, Y., Hong, P. K. A., and Wavrek, D. A.: Integrated chemical-biological treatment of benzo[a]pyrene,
287 Environmental Science & Technology, 34, 854-862, https://doi.org/10.1021/es990817w, 2000b.
288 Zimmerman, A. R.: Abiotic and microbial oxidation of laboratory-produced black carbon (biochar),
289 Environmental Science & Technology, 44, 1295-1301, https://doi.org/10.1021/es903140c, 2010.
290 Zimmerman, A. R., Gao, B., and Ahn, M.-Y.: Positive and negative carbon mineralization priming effects among
291 a variety of biochar-amended soils, Soil Biology & Biochemistry, 43, 1169-1179,
292 https://doi.org/10.1016/j.soilbio.2011.02.005, 2011.